Electronic Supplementary Information

Ultrafast Energy and Electron Transfers in Structurally Well Addressable BODIPY-Porphyrin-Fullerene Polyads

Di Gao, Shawkat M. Aly, Paul-Ludovic Karsenti, Gessie Brisard and Pierre D. Harvey*

Table of Content

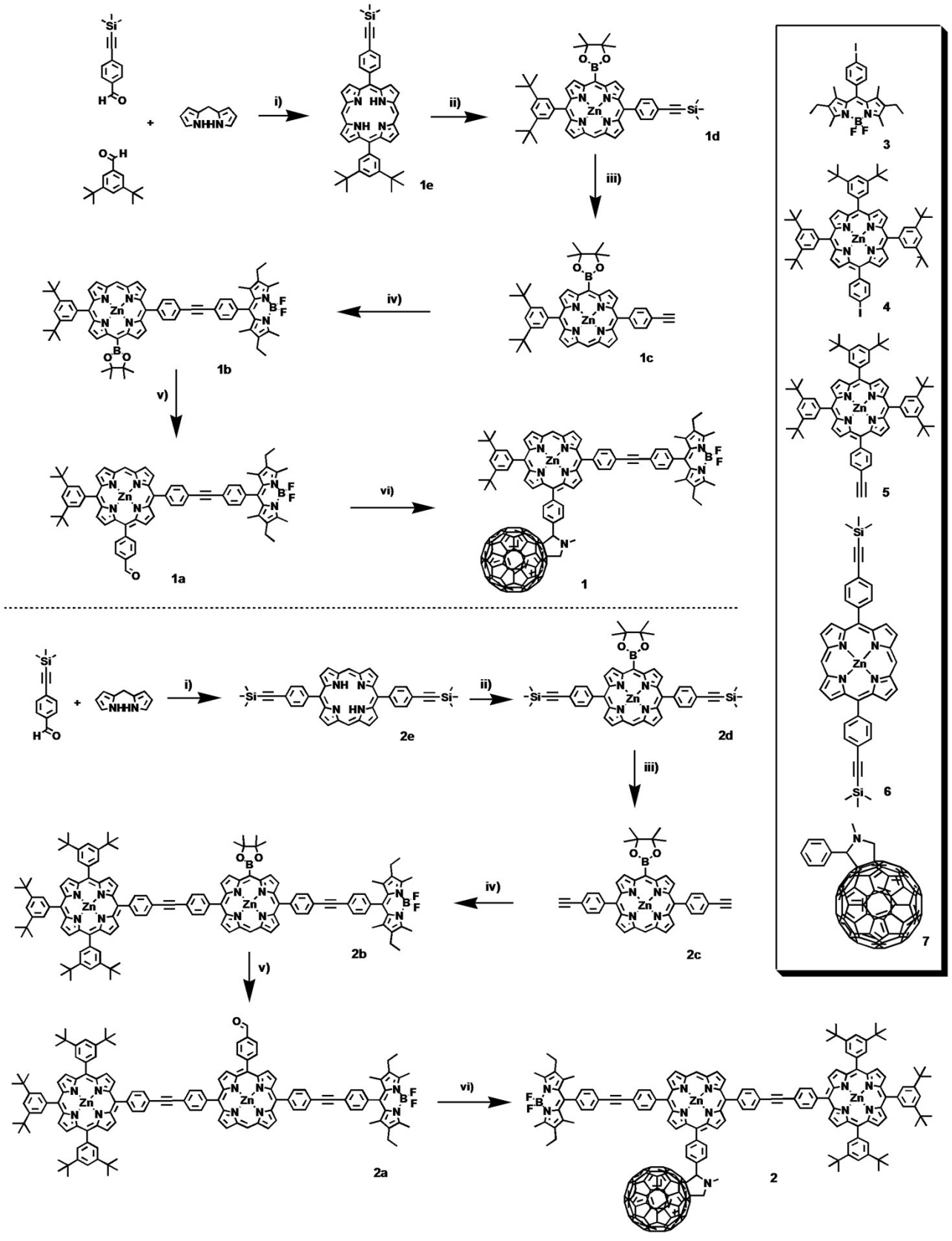

Scheme 1. Synthesis of [BODIPY]-[ZnP]-[C60] dyads: (i) $BF_3{\cdot}Et_2O$, DDQ; (ii) 1. NBS (**1e/2e-Br**), 2. $Zn(OAc)_2{\cdot}2H_2O$(**1e/2e-ZnBr**), 3. Pinacolborane, $PdCl_2(PPh_3)_2$, TEA; (iii) TBAF; (iv) **3** (for compound **1b**)/ **3** and **4** (for compound **2b**), $Pd_2(dba)_3$, $AsPh_3$; (v) 4-bromobenzaldehyde, $Pd(PPh_3)_4$, Cs_2CO_3; vi) sarcosine, fullerene.

Electrochemistry.

The electrochemical measurements were carried out using a PAR 273A potentiostat. The supporting electrolyte was 0.1 M tetra-n-butylammonium hexafluorophosphate ($TBAPF_6$) in anhydrous DCM. The salt was obtained from Sigma-Aldrich and used without further purification. The measurements were performed in a three-compartment electrochemical cell. A platinum wire was employed as the counter electrode, and a freshly polished silver wire as a pseudoreference electrode. Ferrocene (Fc) was added as an internal reference, and all the potentials were referenced relative to the Fc/Fc^+ couple. A glassy carbon disk (0.07 cm^2) was used as the working electrode which was polished with alumina (0.3 μm) on felt pads (Buehler) and treated ultrasonically for 1 min before each experiment. All electrochemical measurements were carried out under a flow of argon and performed at room temperature. The scan rate for cyclic voltammetry (CV) was 100 mV/s.

For the reference **1a**, it shows three reversible one-electron oxidation process at 0.41, 0.60, and 0.74 V versus Fc/Fc^+, the first and third ones can be attributed to be the oxidation of $[ZnP]_c$ unit based on reference **6** and the second oxidation process can be assigned as the oxidation of [BODIPY] moiety based on reference **3**. For **2a**, the CV shows four reversible 1-electron oxidation processes at 0.31, 0.45, 0.63 and 0.78 V *vs* Fc/Fc^+. The first 1-electron oxidation process can be attributed to $[ZnP]_t$ based on reference **5**. The second 1-electron process can be assigned to be the oxidation of $[ZnP]_c$ and the third oxidation peak appears to be the oxidation of [BODIPY] based on reference **3**. The fourth peak can be attributed to the overlapping oxidation of both $[ZnP]_t$ and $[ZnP]_c$. On the reduction side, both **1a** and **2a**, show two reversible reduction processes. For both of them, the first 1-electron reduction process can be the assigned as the overlapping reduction of [BODIPY] and the first reduction of $[ZnP]_t$ and $[ZnP]_c$.[1] The second reduction process of them can be attributed to be the second reduction process of $[ZnP]_t$ and $[ZnP]_c$.

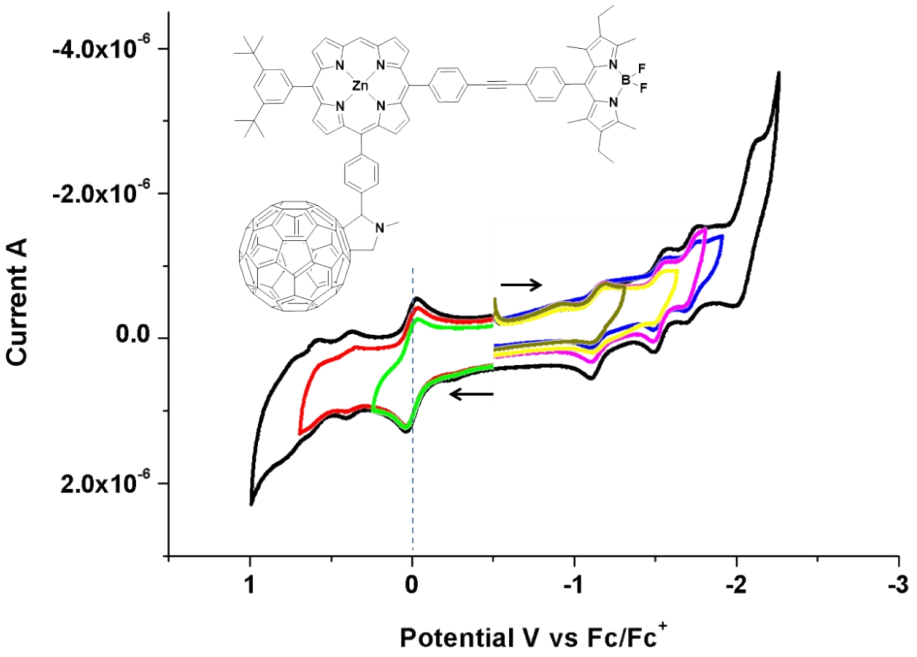

Figure S1. Cyclic voltammograms of **1** in DCM, 0.1 M $TBAPF_6$. Scan rate = 100 mV/s.

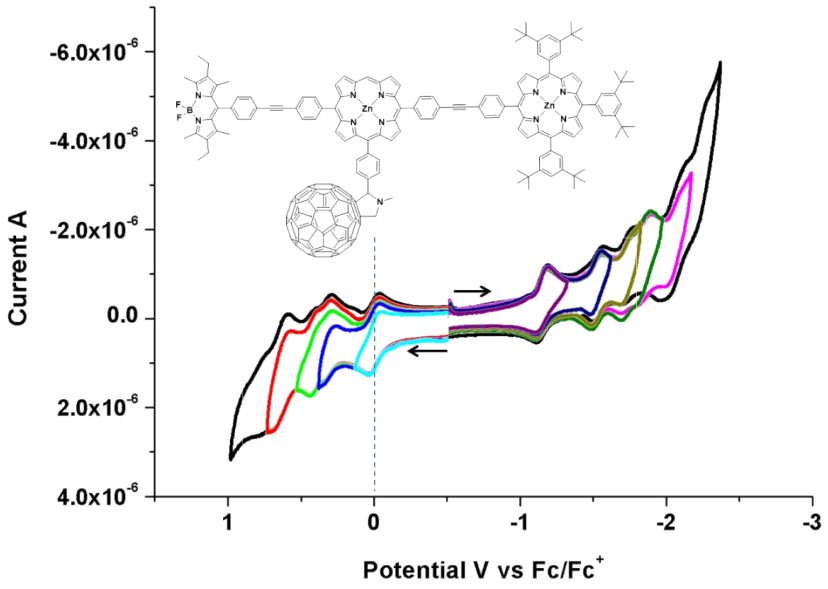

Figure S2. Cyclic voltammograms of **2** in DCM, 0.1 M $TBAPF_6$. Scan rate = 100 mV/s.

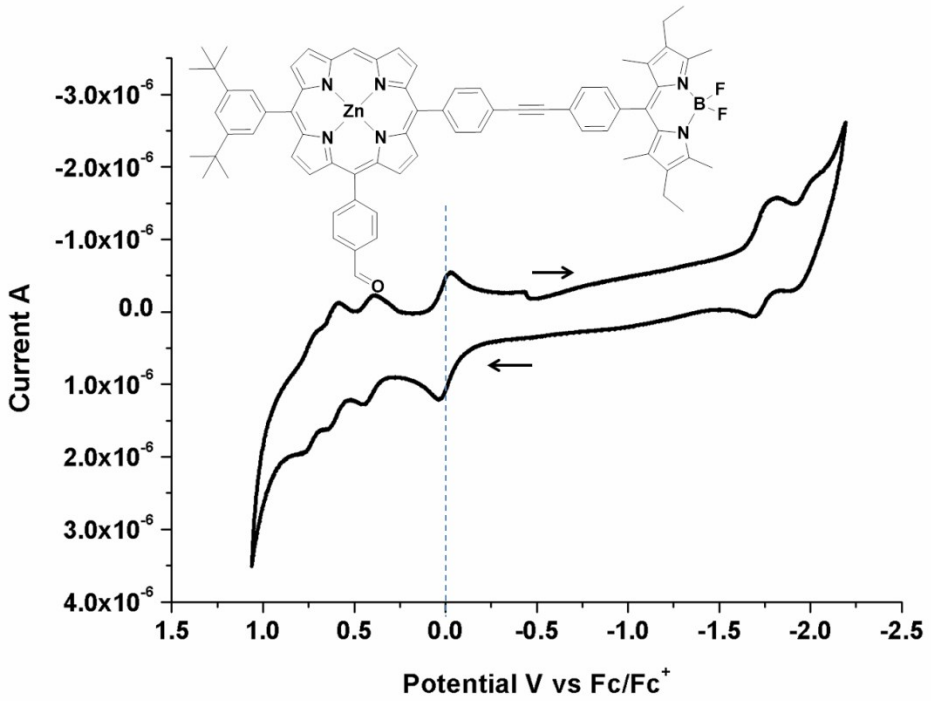

Figure S3. Cyclic voltammograms of **1a** in DCM, 0.1 M $TBAPF_6$. Scan rate = 100 mV/s.

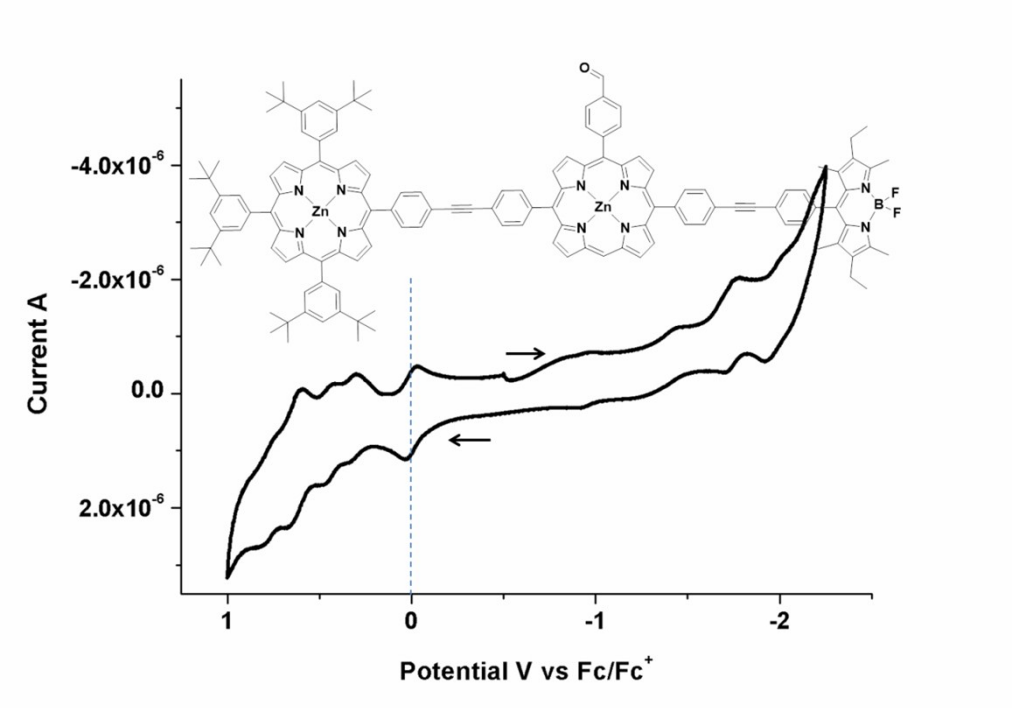

Figure S4. Cyclic voltammograms of **2a** in DCM, 0.1 M $TBAPF_6$. Scan rate = 100 mV/s.

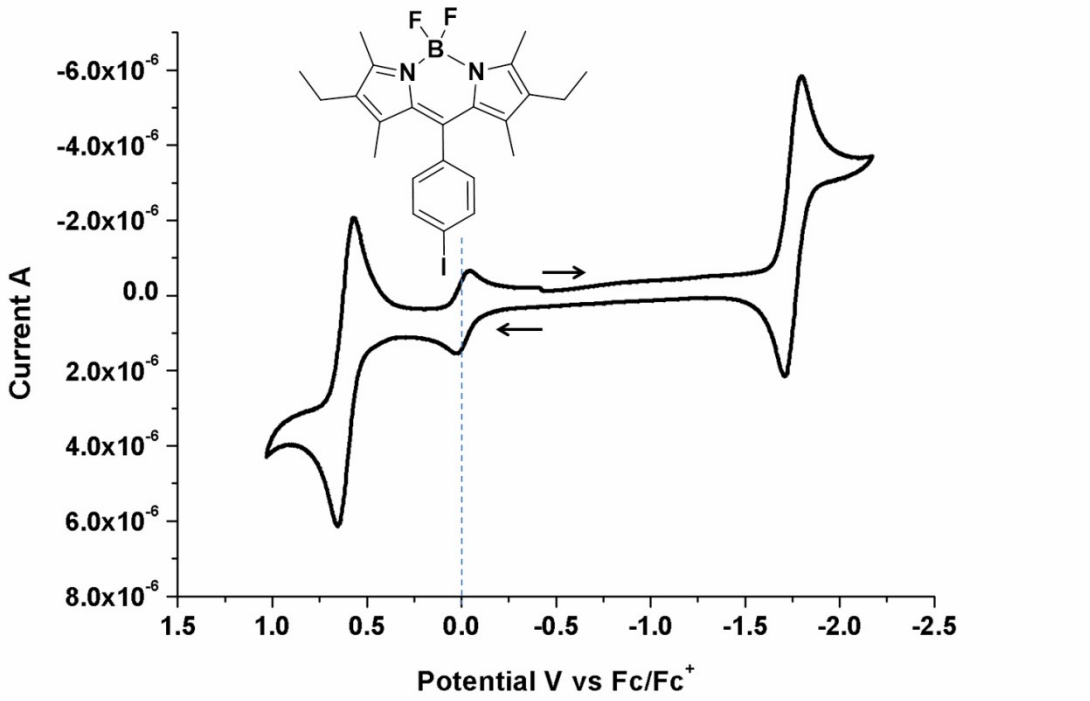

Figure S5. Cyclic voltammograms of **3** in DCM, 0.1 M $TBAPF_6$. Scan rate = 100 mV/s.

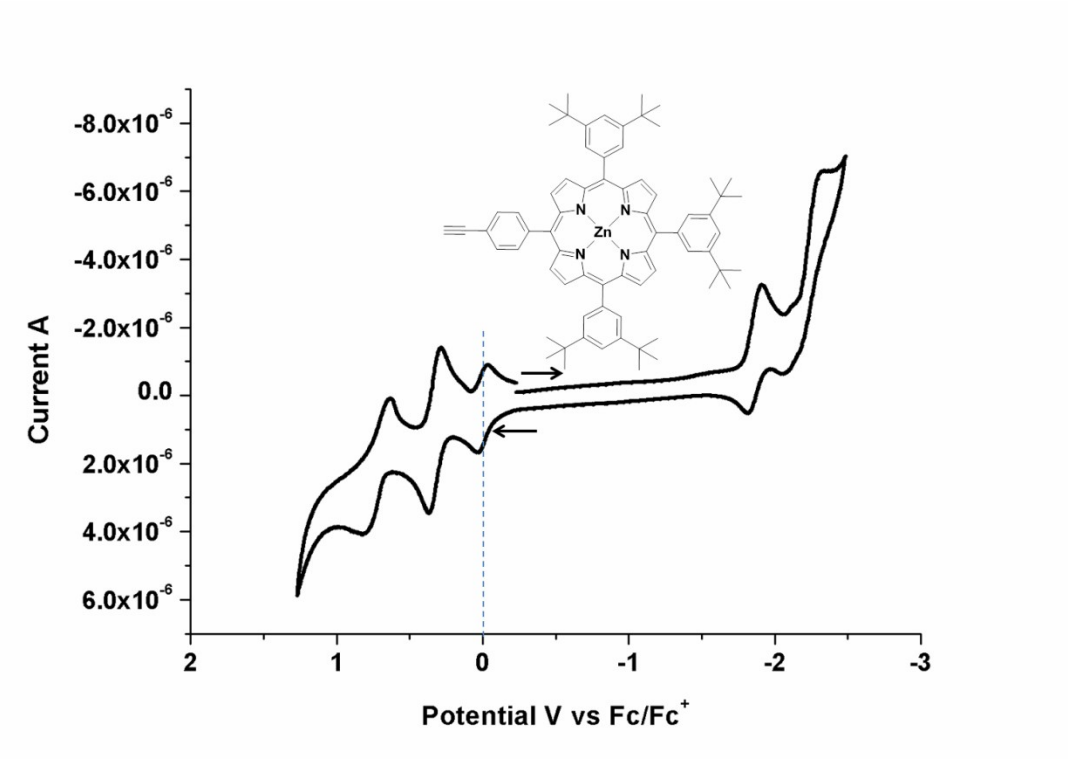

Figure S6. Cyclic voltammograms of **5** in DCM, 0.1 M $TBAPF_6$. Scan rate = 100 mV/s.

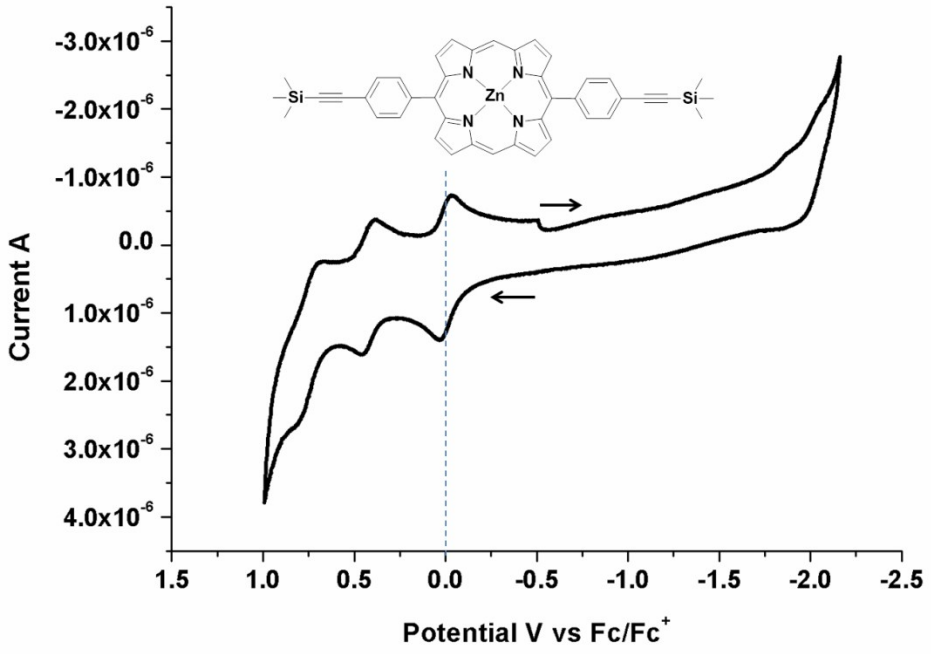

Figure S7. Cyclic voltammograms of **6** in DCM, 0.1 M $TBAPF_6$. Scan rate = 100 mV/s.

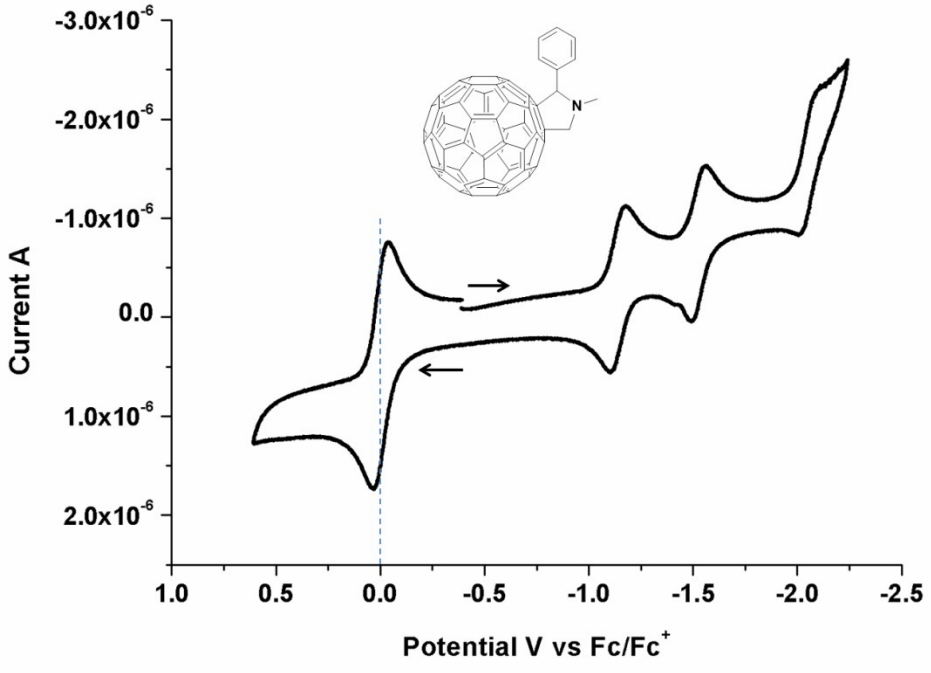

Figure S8. Cyclic voltammograms of **7** in DCM, 0.1 M $TBAPF_6$. Scan rate = 100 mV/s.

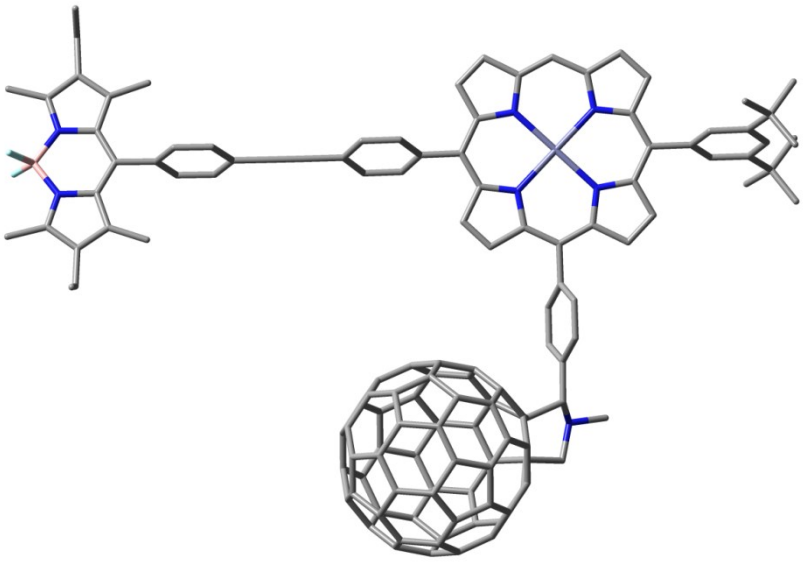

Figure S9. Geometry optimization of **1** (DFT; B3LYP).

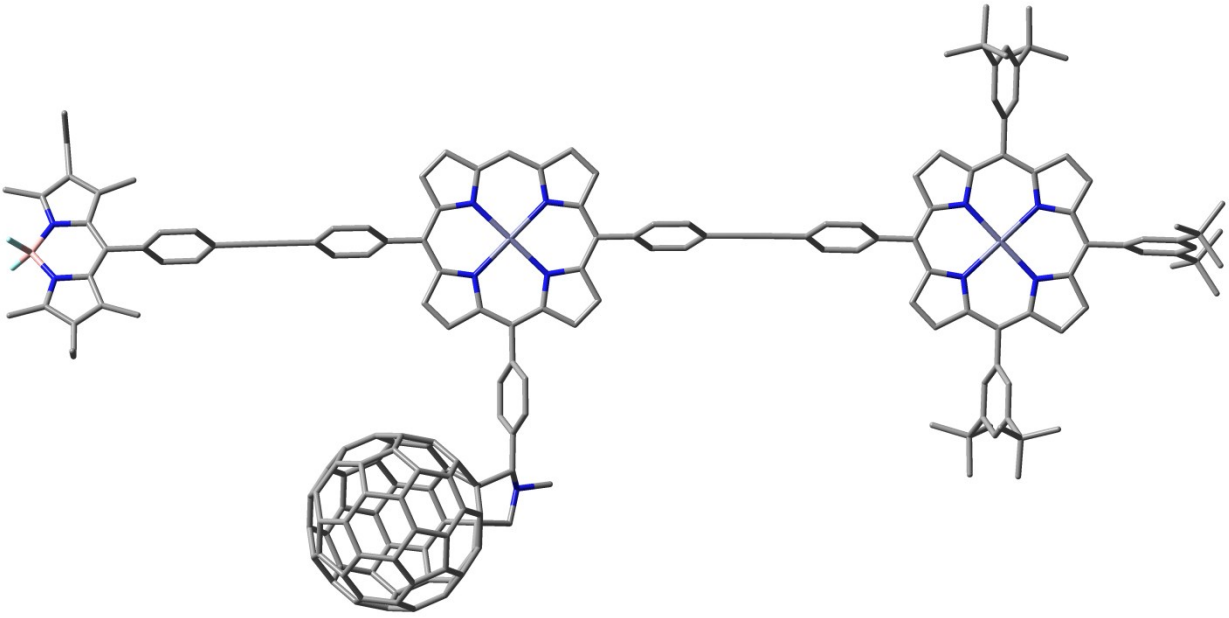

Figure S10. Geometry optimization of **2** (DFT; B3LYP).

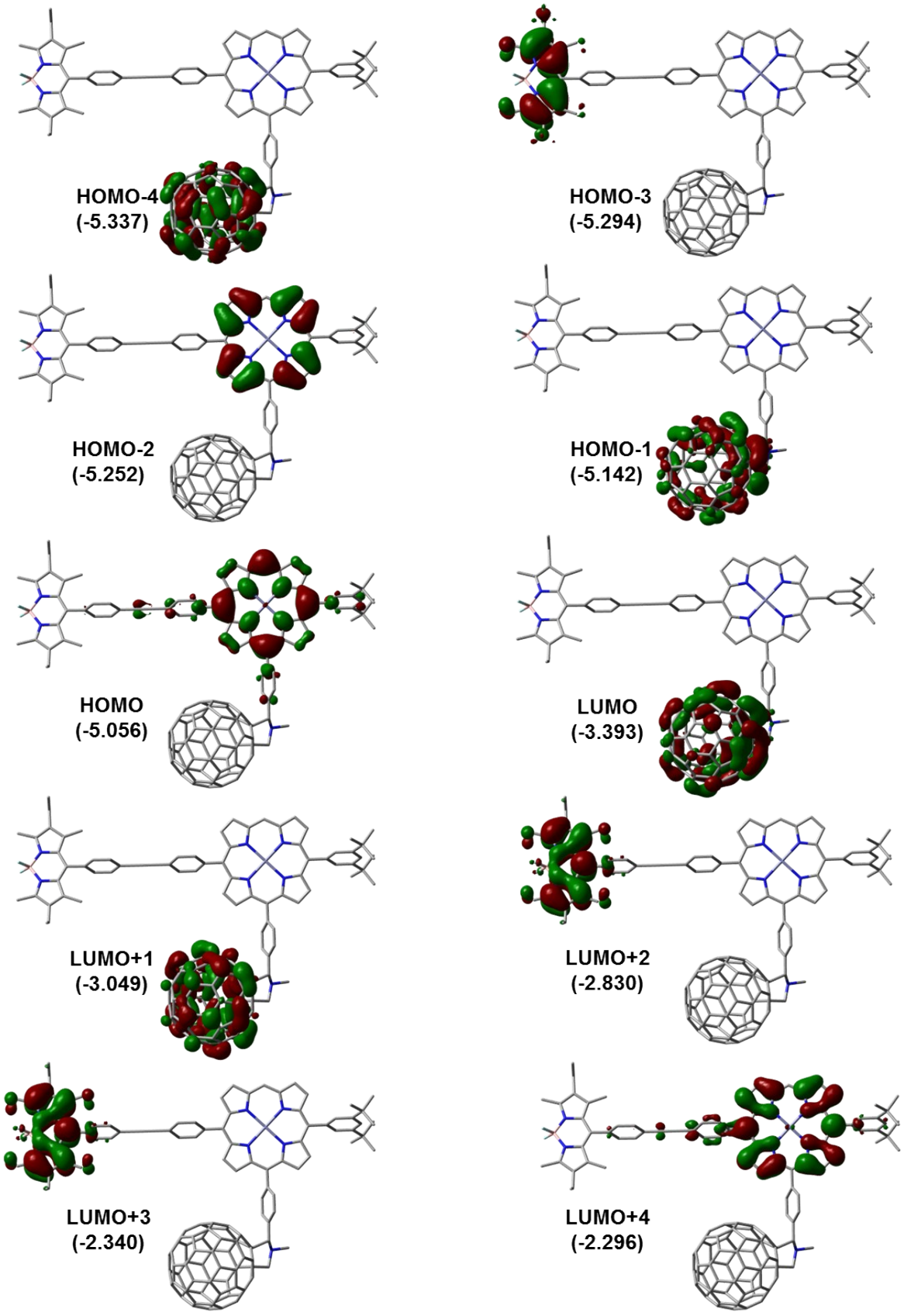

Figure S11. MO representations after geometry optimization of the frontier MOs for **1**; energies in eV.

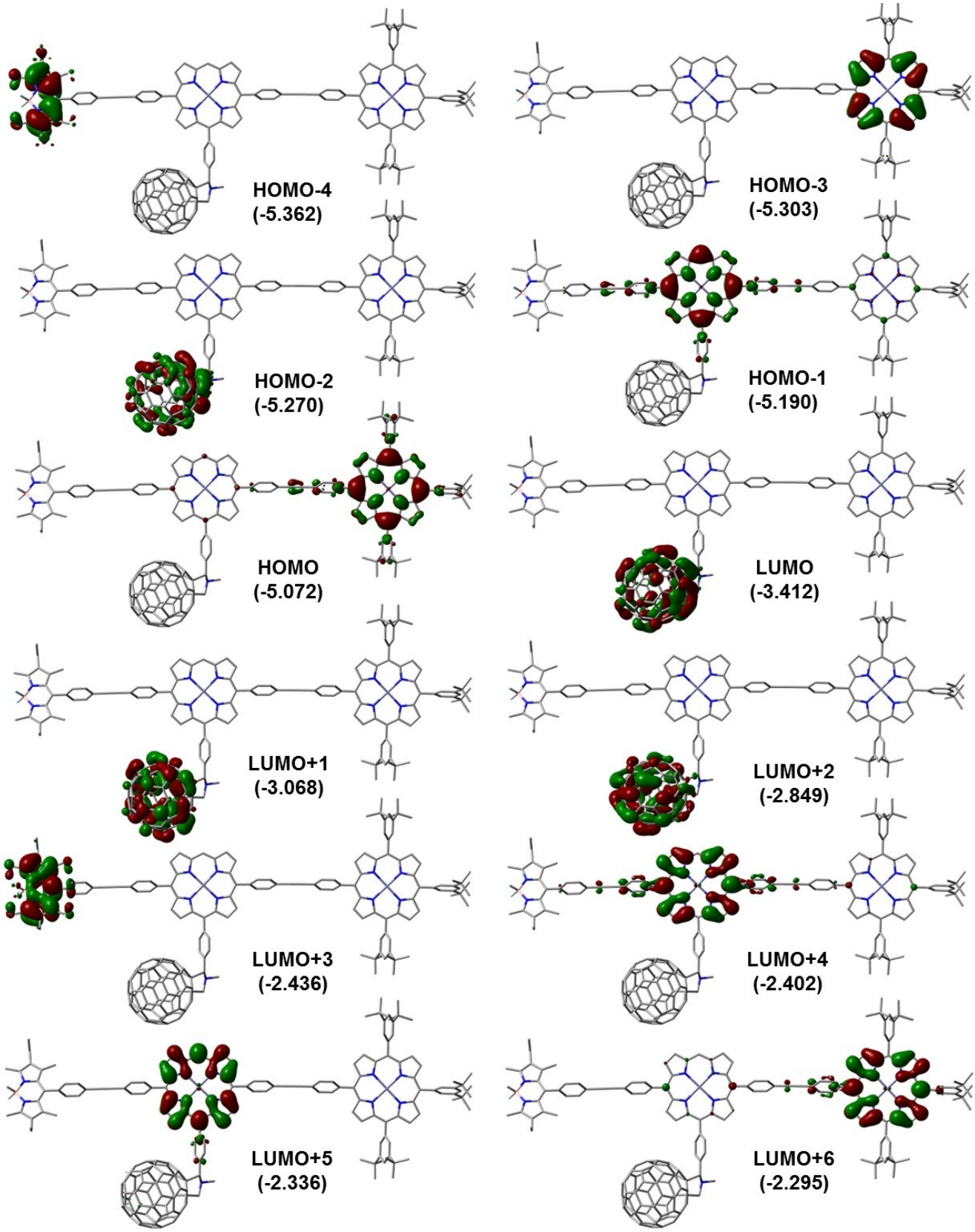

Figure S12. MO representations after geometry optimization of the frontier MOs for **2**; energies in eV.

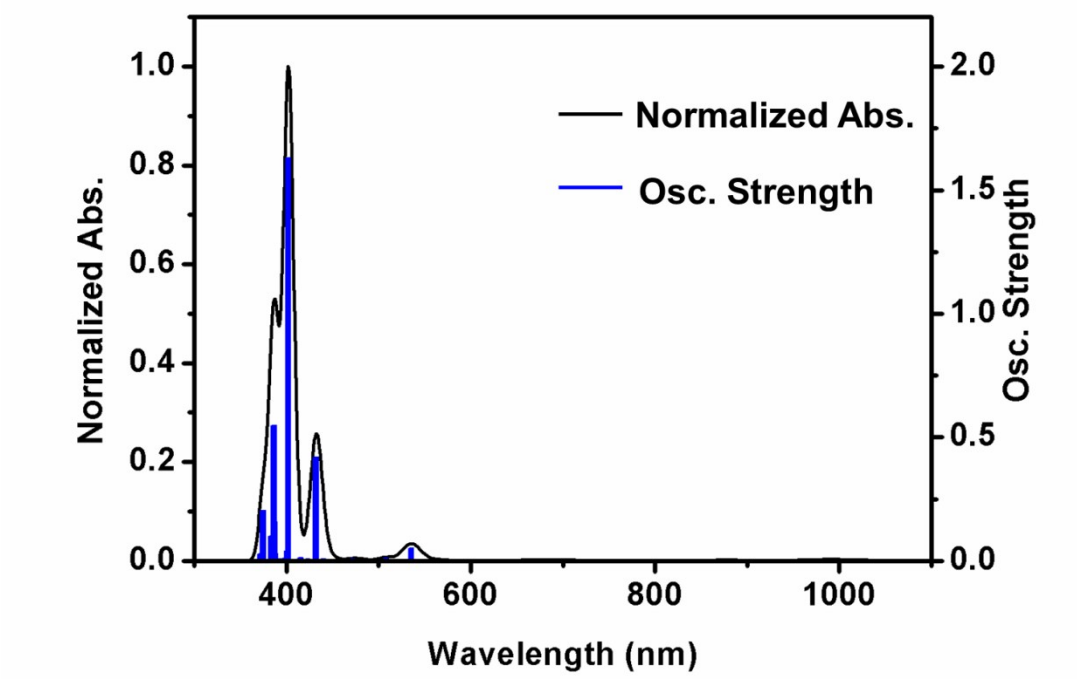

Figure S13. Bar graph reporting the calculated oscillator strength and calculated position of the 100st electronic transitions calculated by TDDFT for **1** (bar graph; f = computed oscillator strength). The black line is generated by assigning an arbitrary thickness of 1000 cm^{-1} to each bar.

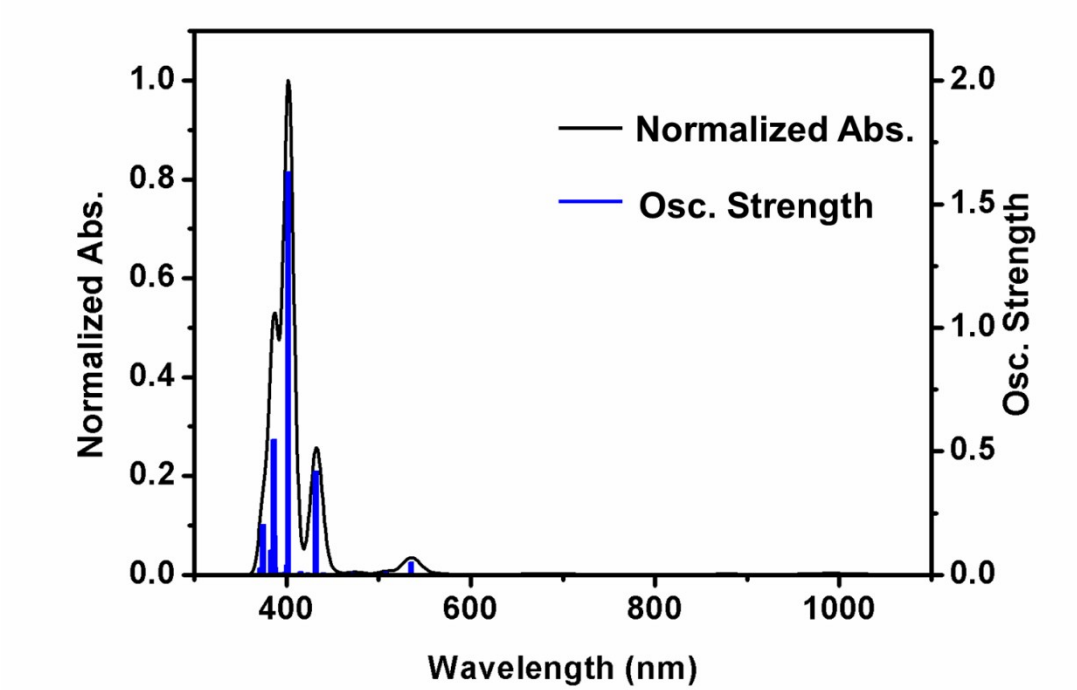

Figure S14. Bar graph reporting the calculated oscillator strength and calculated position of the 100st electronic transitions calculated by TDDFT for **2** (bar graph; f = computed oscillator strength). The black line is generated by assigning an arbitrary thickness of 1000 cm^{-1} to each bar.

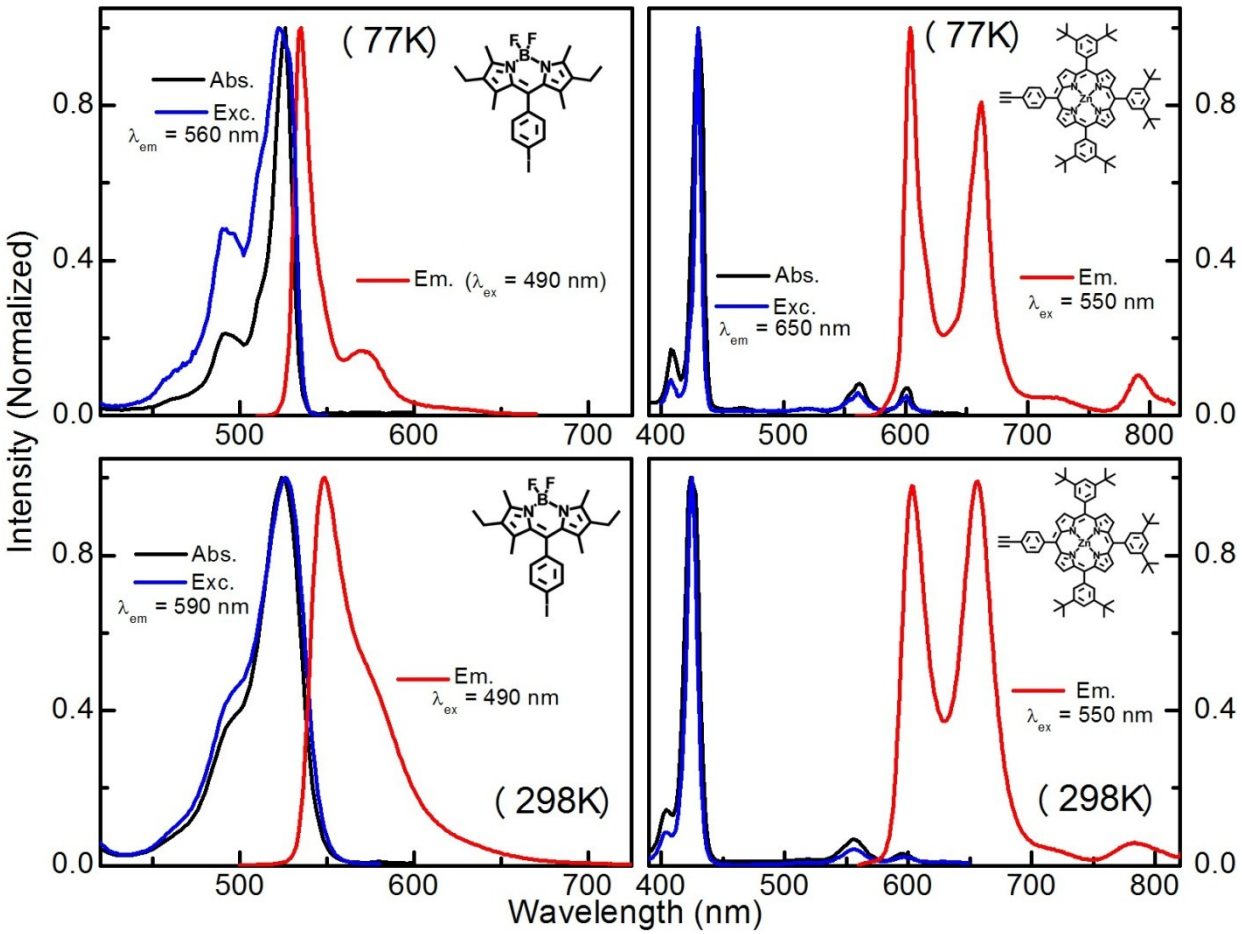

Figure S15. Absorption (black), excitation (blue), and emission (red) of **3** and **5** in 2MeTHF at 77 K (up) and 298 K (down). Wavelengths used for the measurements are indicated on the graph.

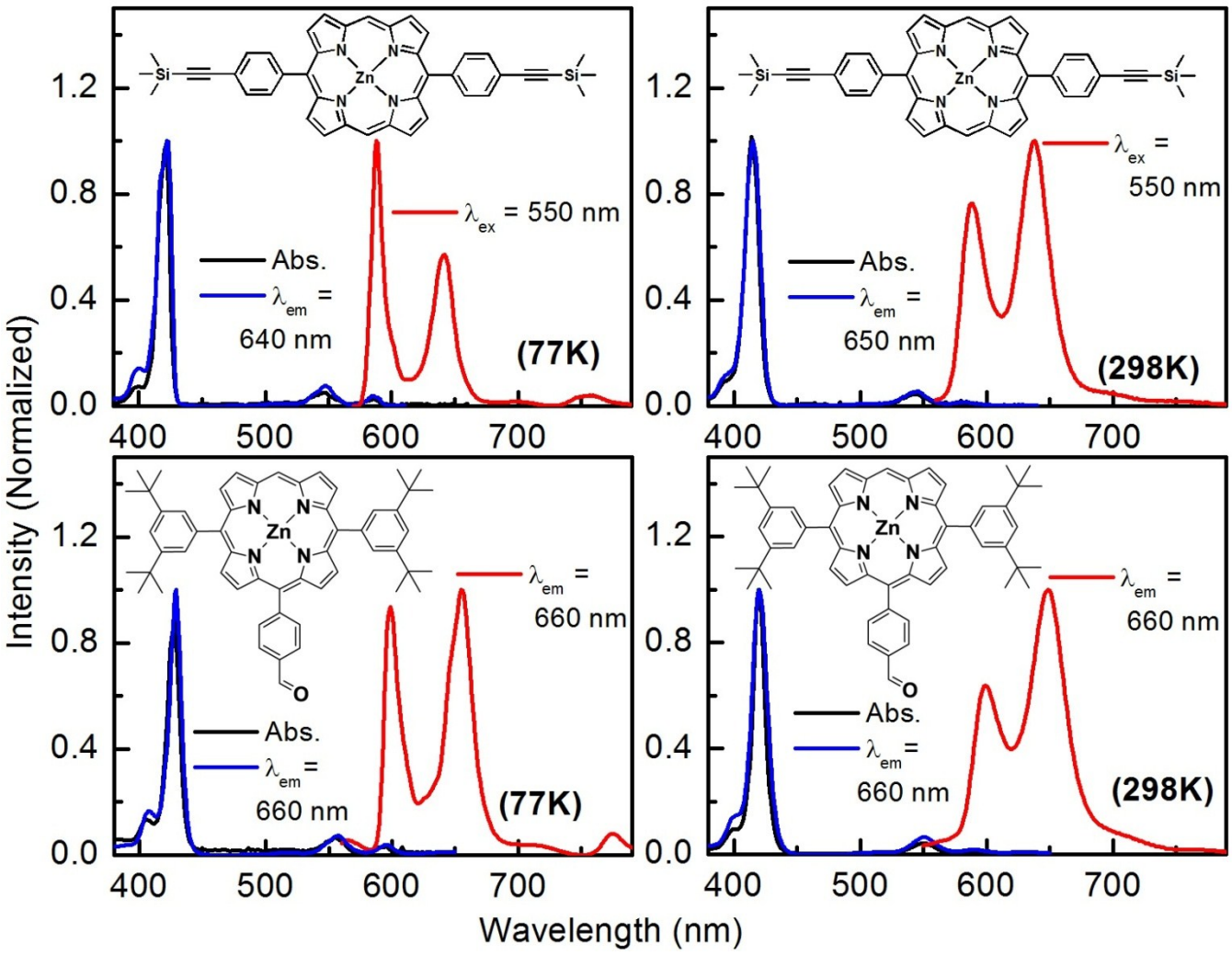

Figure S16. Absorption (black), excitation (blue), and emission (red) of **6** (up) and **8** (down) in 2MeTHF at 77 K and 298 K. Wavelengths used for the measurements are indicated on the graph.

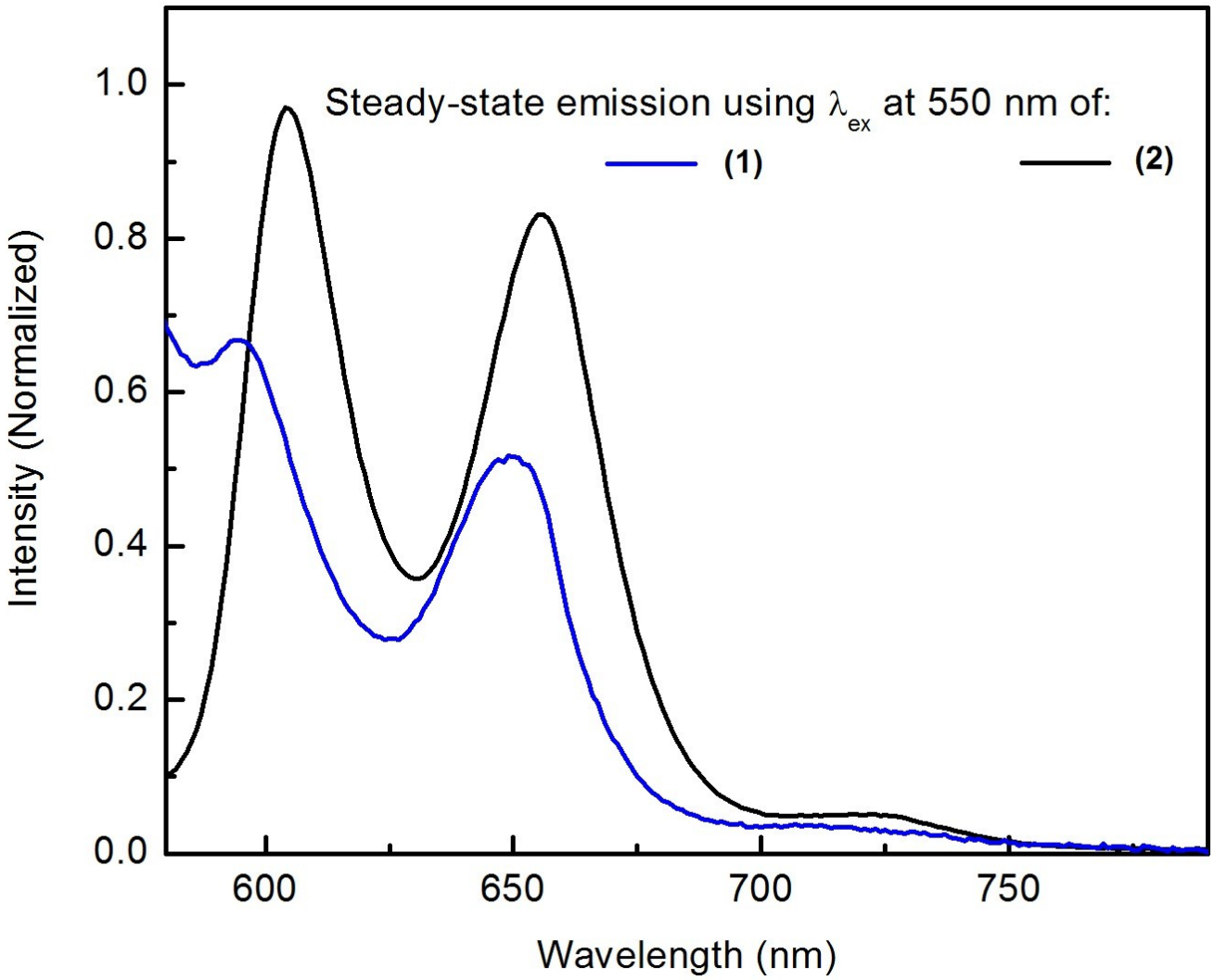

Figure S17. Steady-state emission of **1** (blue) and **2** (black) in 2MeTHF at 298 K (λ_{ex} = 550 nm).

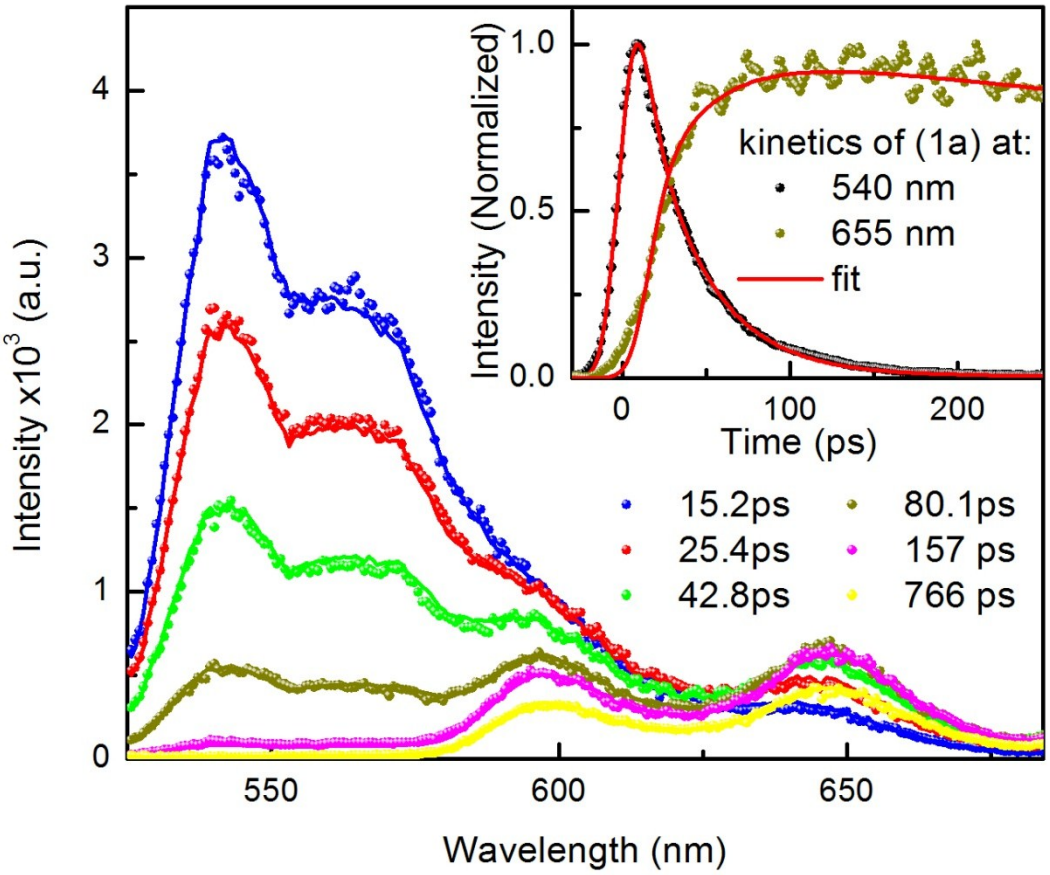

Figure S18. Time-resolved fluorescence measurements (Streak camera; λ_{ex} = 490 nm, pulse width ~100 fs) and kinetic profiles (insets) for **1a** in 2MeTHF at 298 K; delay time are given on the graph. Inset showing kinetic profiles at 540 and 655 nm.

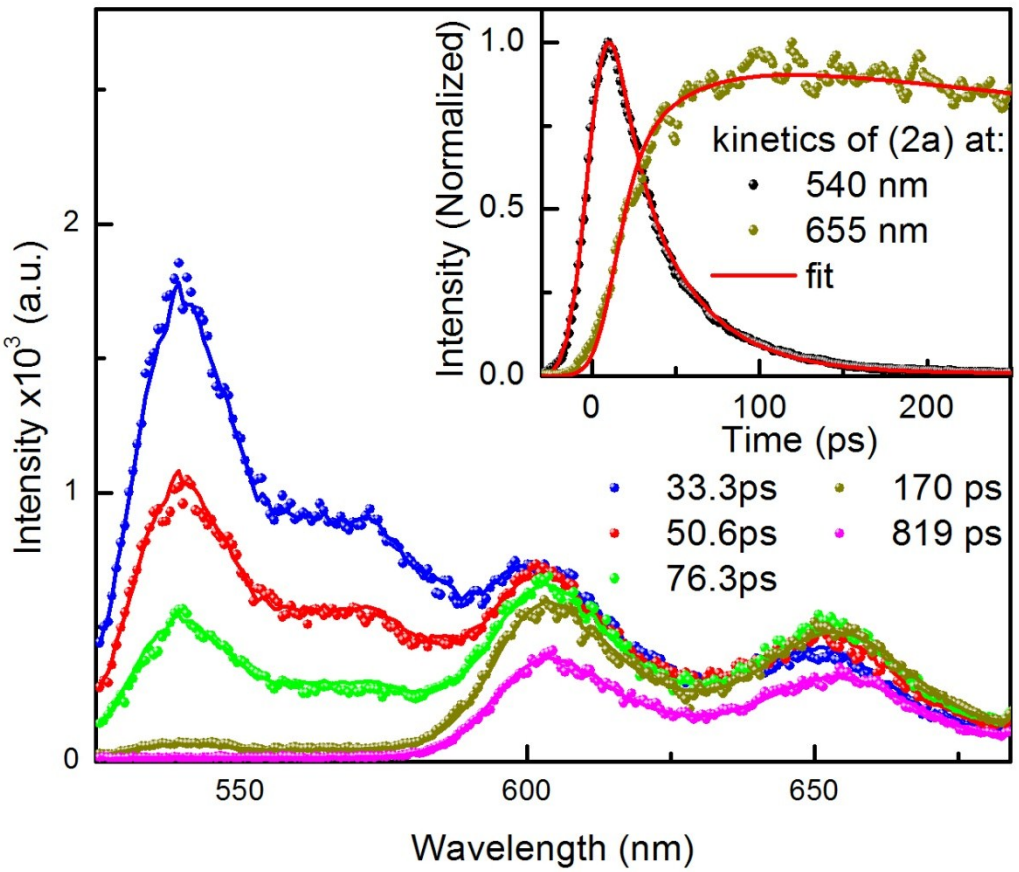

Figure S19. Time-resolved fluorescence measurements (Streak camera; λ_{ex} = 490 nm, pulse width ~100 fs) and kinetic profiles (insets) for **2a** in 2MeTHF at 298 K; delay time are given on the graph.

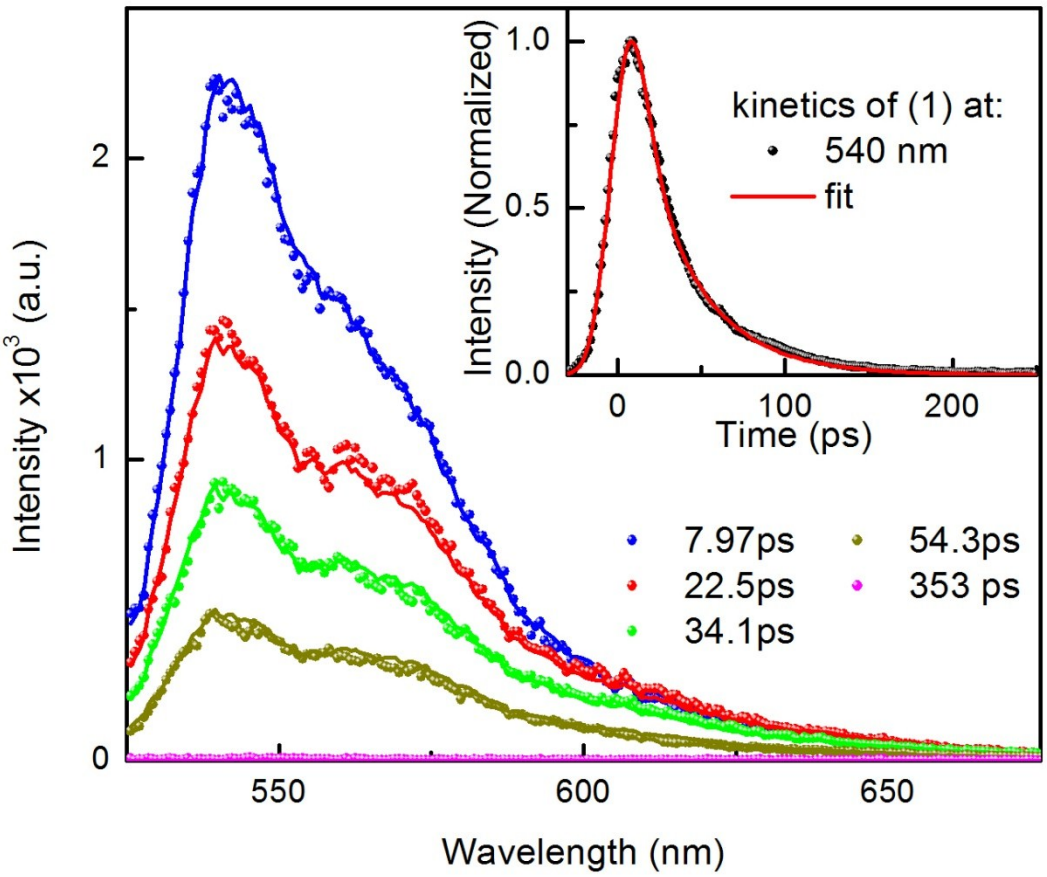

Figure S20. Time-resolved fluorescence measurements (Streak camera; λ_{ex} = 490 nm, pulse width ~100 fs) and kinetic profiles (insets) for **1** in 2MeTHF at 298 K; delay time are given on the graph.

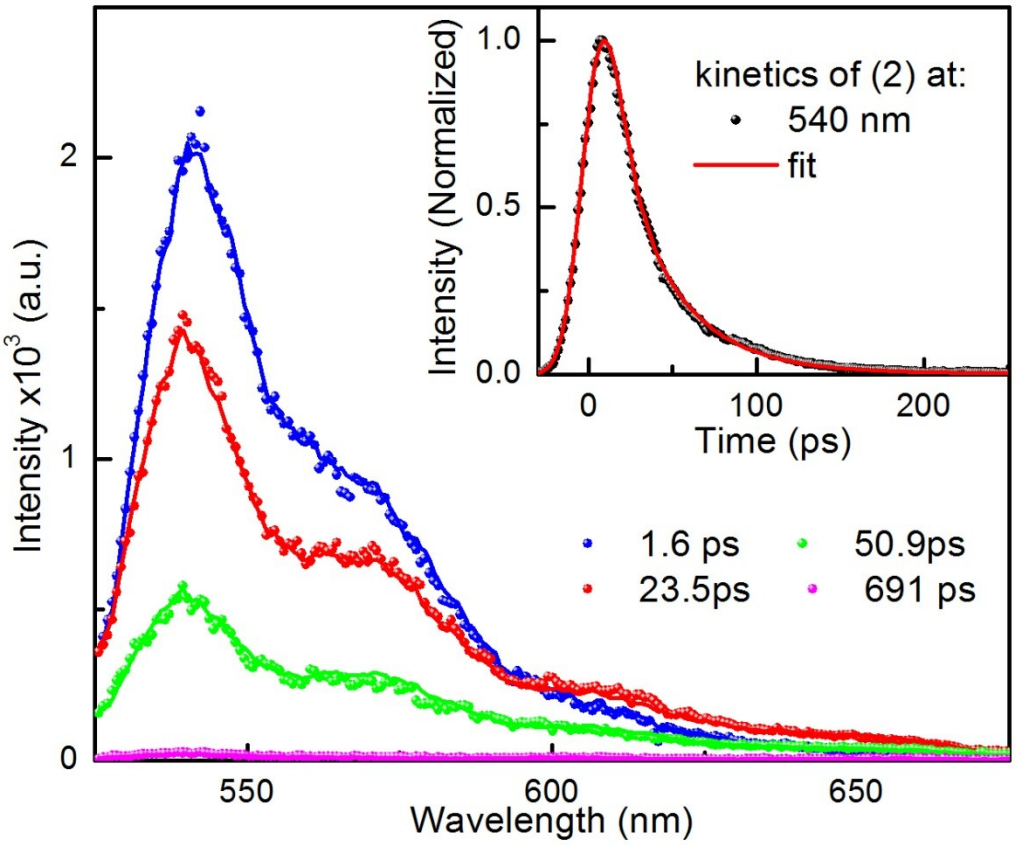

Figure S21. Time-resolved fluorescence measurements (Streak camera; λ_{ex} = 490 nm, pulse width ~100 fs) and kinetic profiles (insets) for **2** in 2MeTHF at 298 K; delay time are given on the graph.

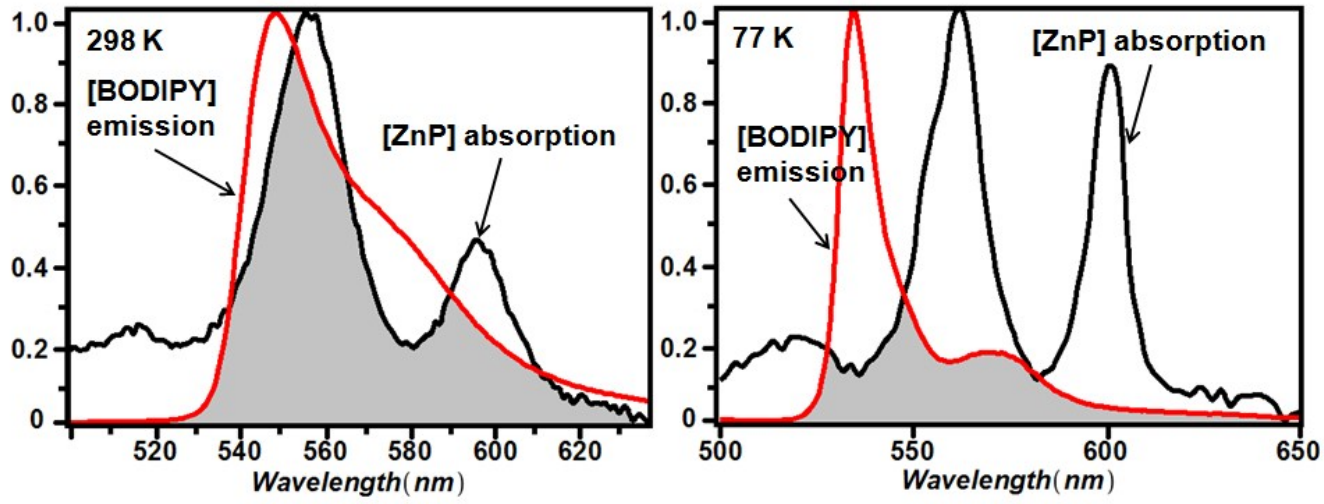

Figure S 22. The overlap integral between BODIPY emission and ZnP absorption in 2MeTHF at 298 K (left) and 77 K (right).

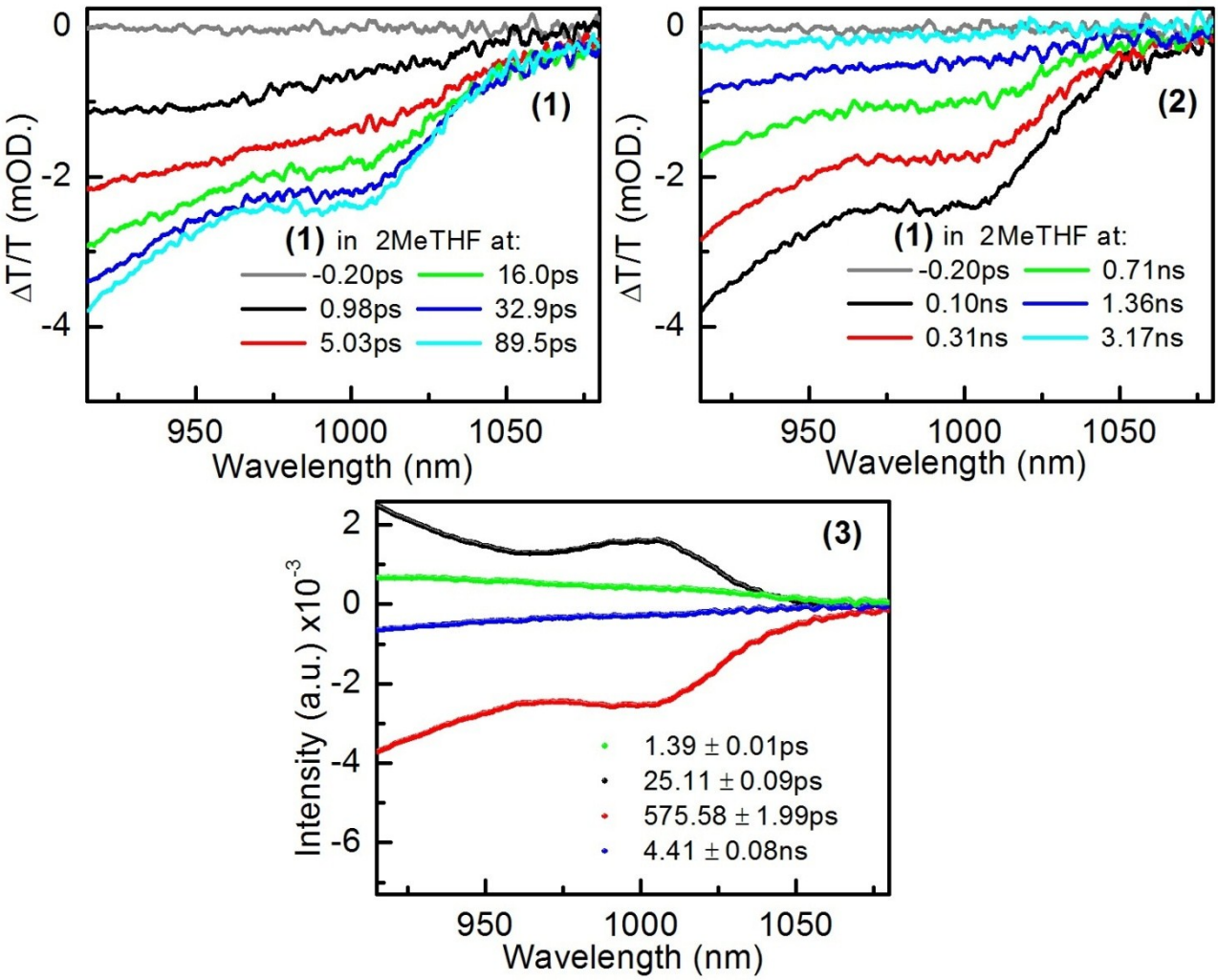

Figure S23. Transient absorption spectra for **1** in 2MeTHF at 298 K: (1) rise, (2) decay, and (3) decay associated spectra (DAS) (λ_{ex} = 525 nm, pulse width ~90 fs). Delay times at which the spectra collected and lifetimes are given on graph.

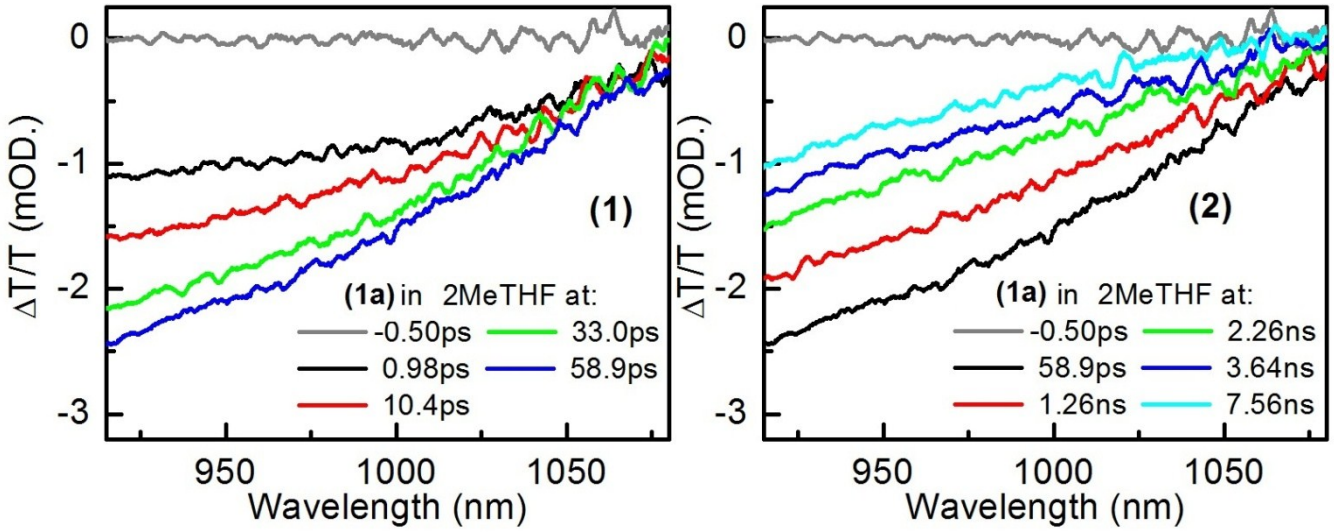

Figure S24. Transient absorption spectra for **1a** in 2MeTHF at 298 K: (1) rise and (2) decay (λ_{ex} = 525 nm, pulse width ~90 fs). Delay times at which the spectra collected are given on the graph.

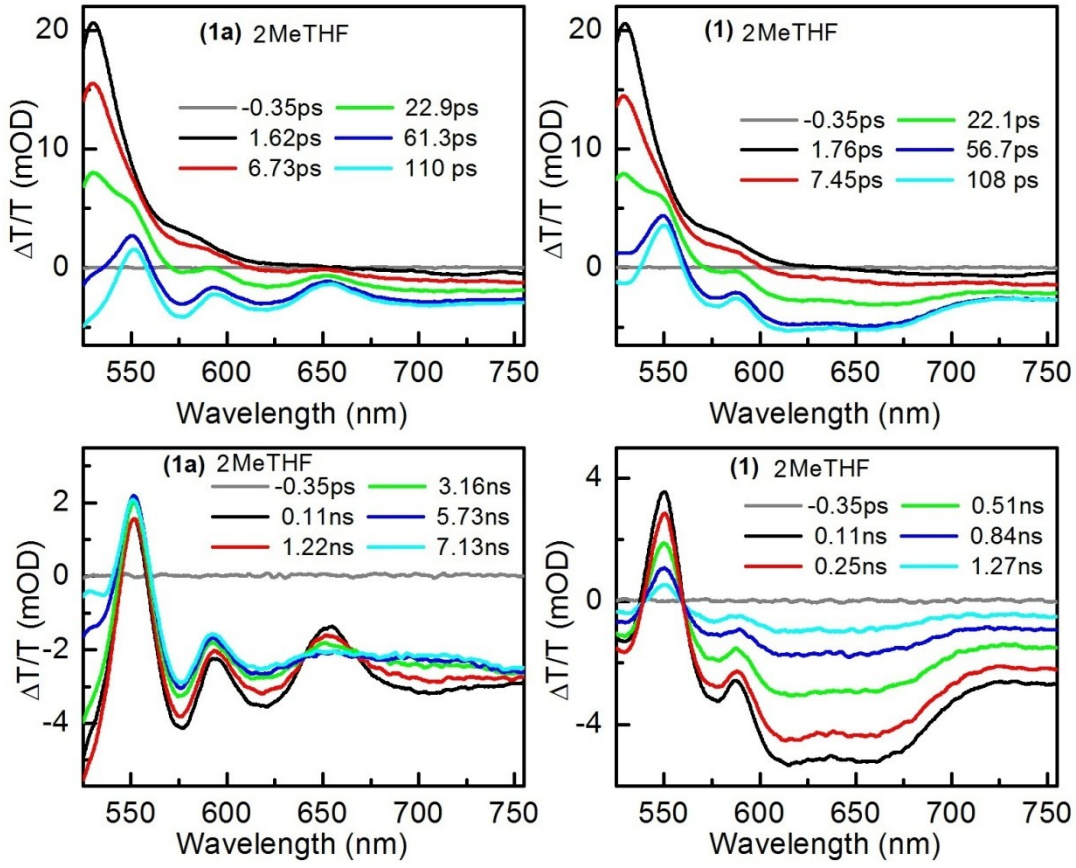

Figure S25. Transient absorption spectra for **1a** (left) and **1** (right) in 2MeTHF at 298 K (λ_{ex} = 525 nm, pulse width ~90 fs). Delay times at which the spectra collected are given on the graph.

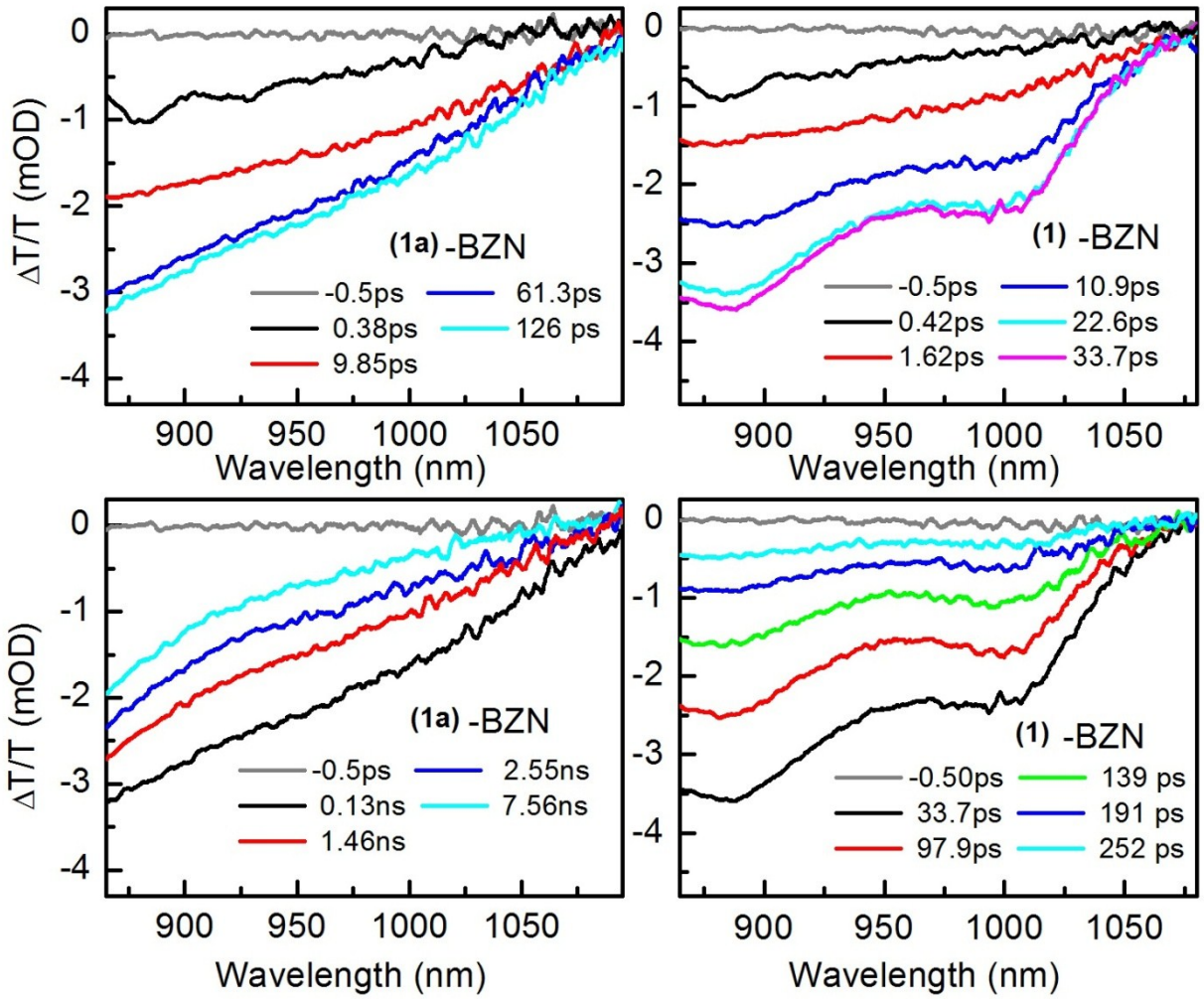

Figure S26. Transient absorption spectra for **1a** (left) and **1** (right) in benzonitrile at 298 K (λ_{ex} = 525 nm, pulse width ~90 fs). Delay times at which the spectra collected are given on the graph.

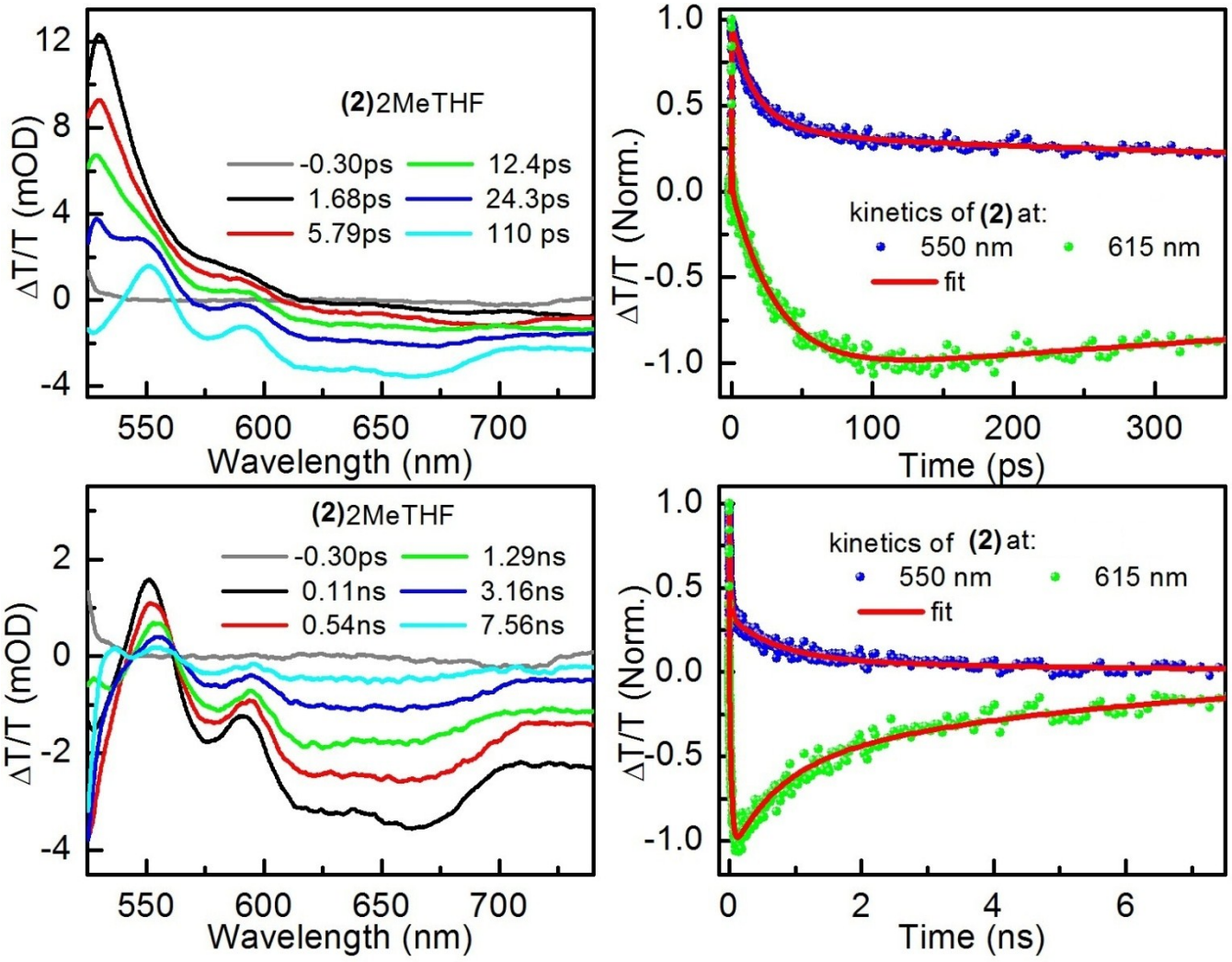

Figure S27. TA spectra (left) and kinetic traces (right) collected for **2** in 2MeTHF at 298 K (λ_{ex} = 525 nm, pulse width ~90 fs). Delay times for TA spectra and monitoring wavelengths for kinetic profile are given on graph and the red lines show the best fitted kinetic traces.

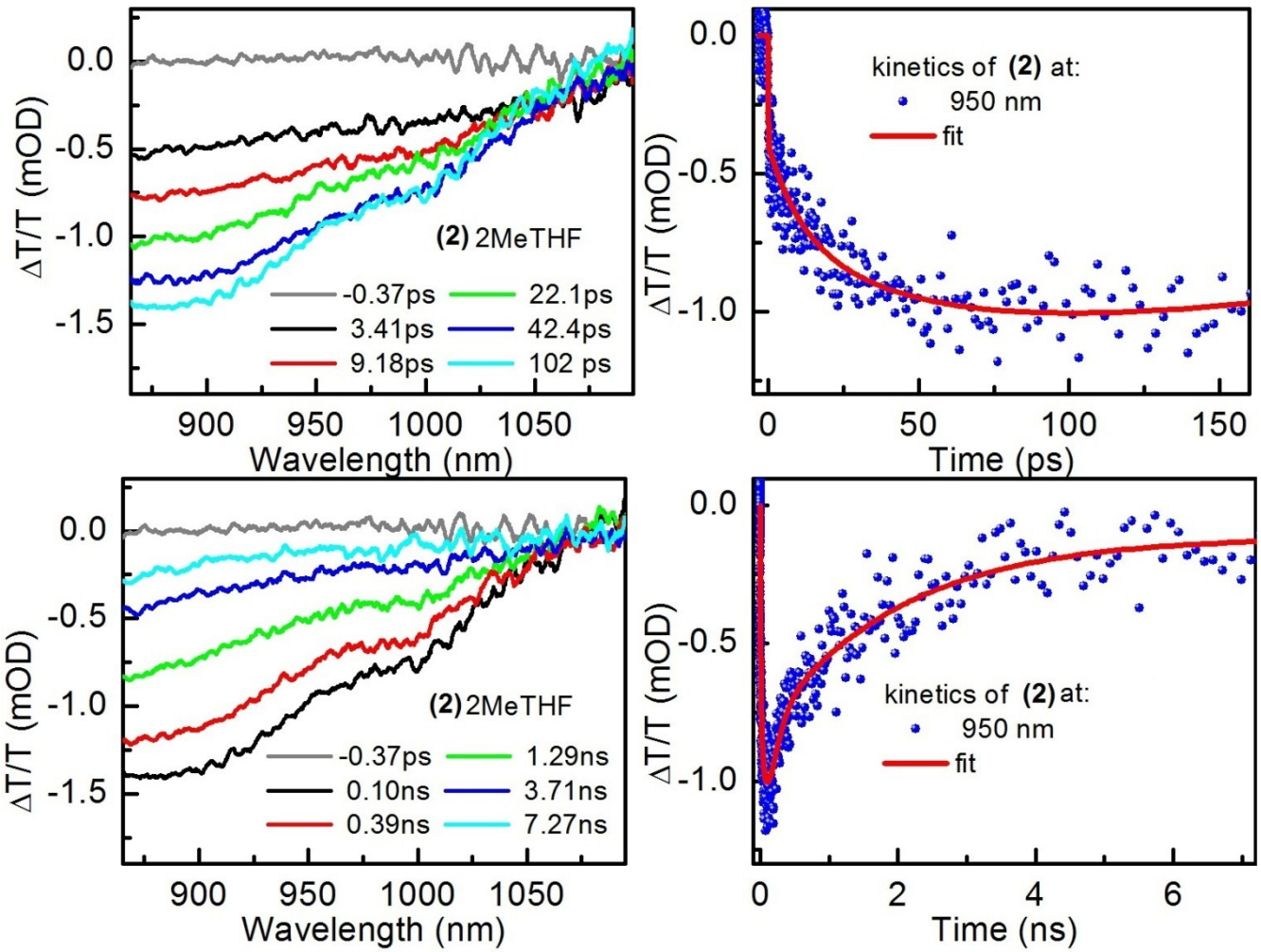

Figure S28. TA spectra (left) and kinetic traces (right) collected for **2** in 2MeTHF at 298 K (λ_{ex} = 525 nm, pulse width ~90 fs). Delay times for TA spectra and monitoring wavelengths for kinetic profile are given on graph and the red lines show the best fitted kinetic traces.

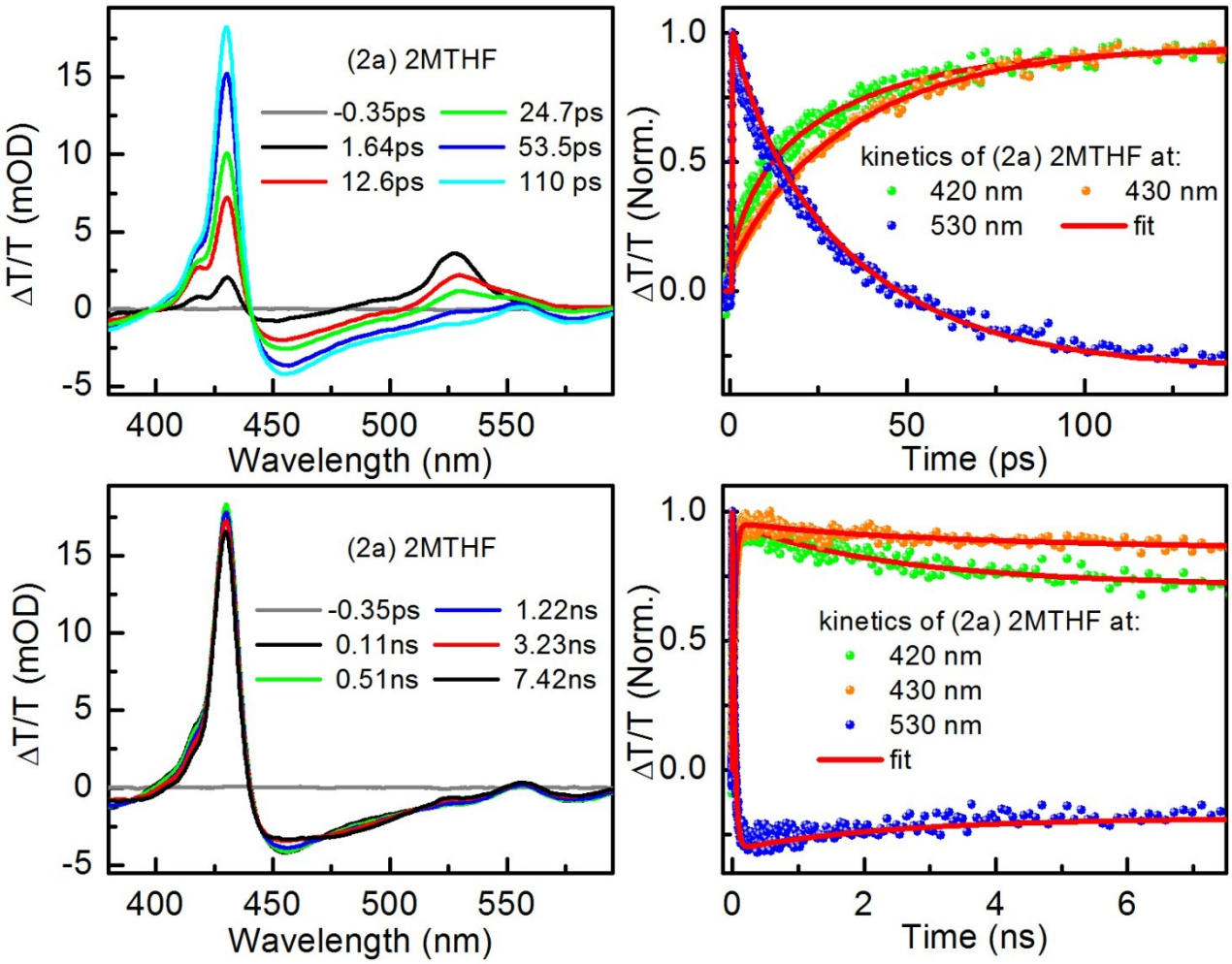

Figure S29. TA spectra (left) and kinetic traces (right) collected for **2a** in 2MeTHF at 298 K (λ_{ex} = 525 nm, pulse width ~90 fs). Delay times for TA spectra and monitoring wavelengths for kinetic profile are given on graph and the red lines show the best fitted kinetic traces.

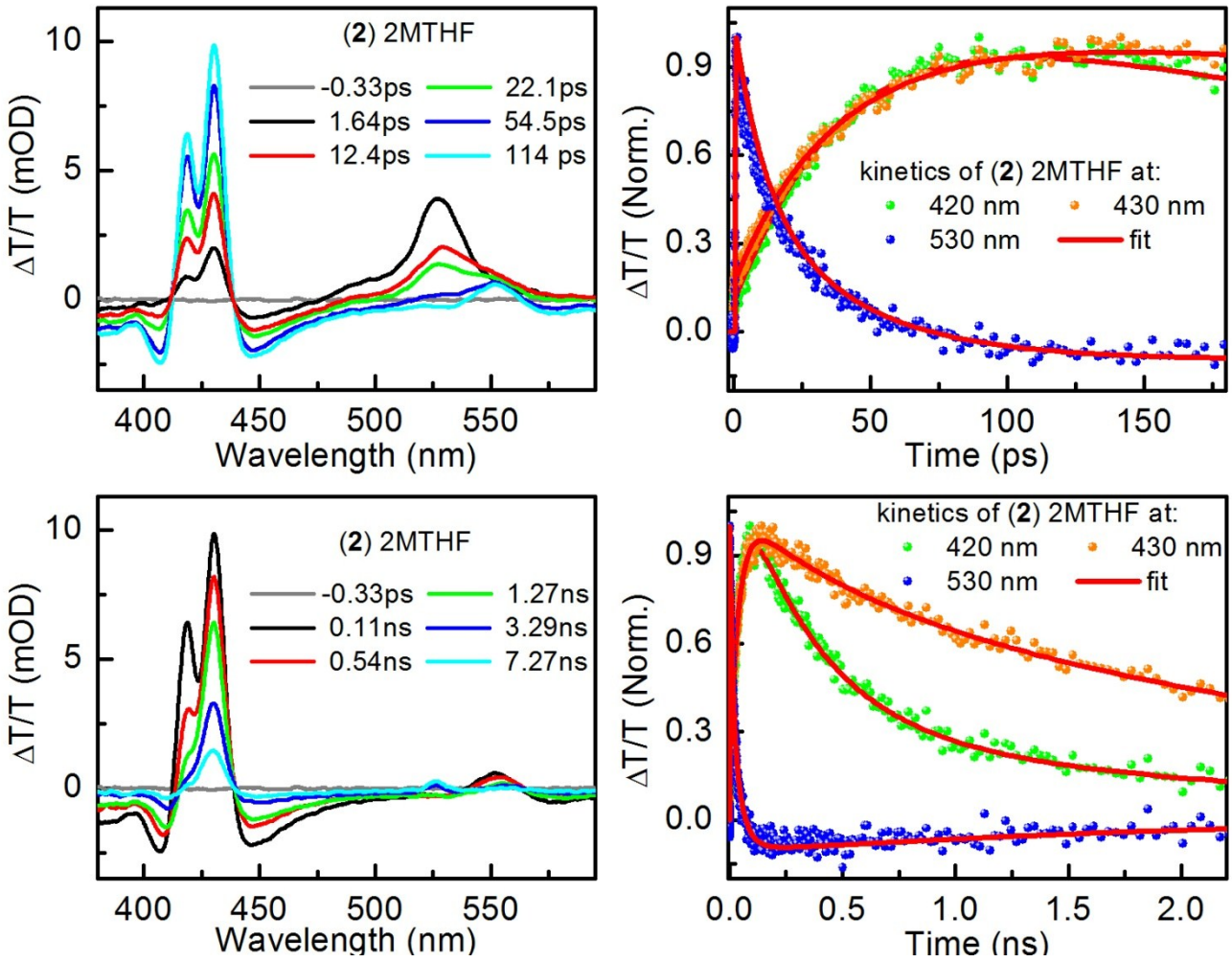

Figure S30. TA spectra (left) and kinetic traces (right) collected for **2** in 2MeTHF at 298 K (λ_{ex} = 525 nm, pulse width ~90 fs). Delay times for TA spectra and monitoring wavelengths for kinetic profile are given on graph and the red lines show the best fitted kinetic traces.

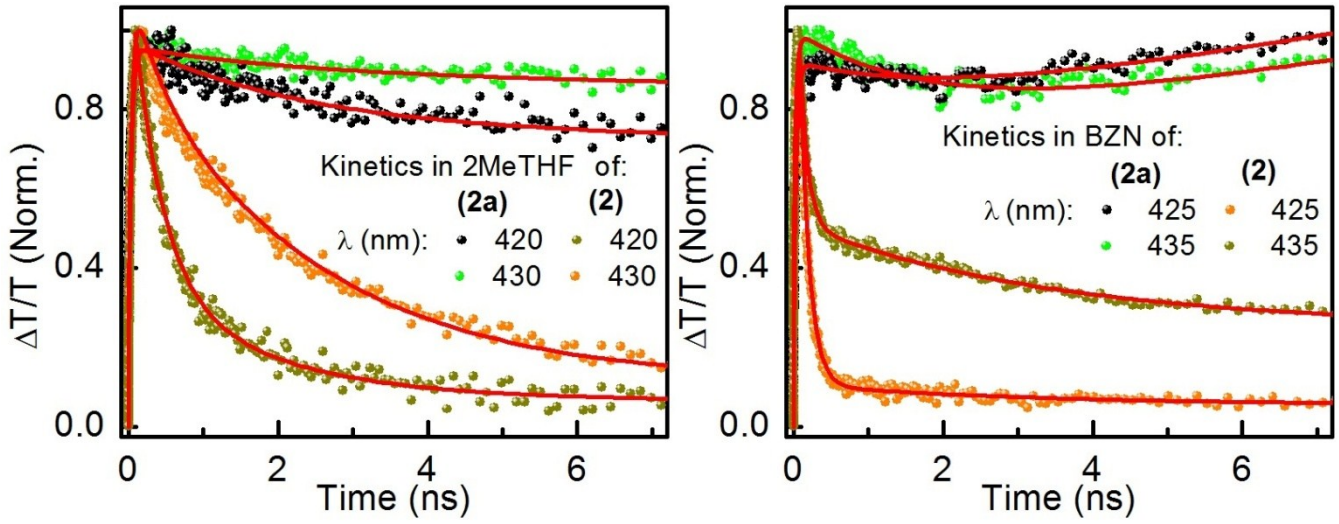

Figure S31. Kinetic traces for **2a** and **2** collected in 2MeTHF (left) and BZN (right) at 298 K (λ_{ex} = 525 nm, pulse width ~90 fs). Monitoring wavelength are given on graph and the red lines show the best fitted kinetic traces.

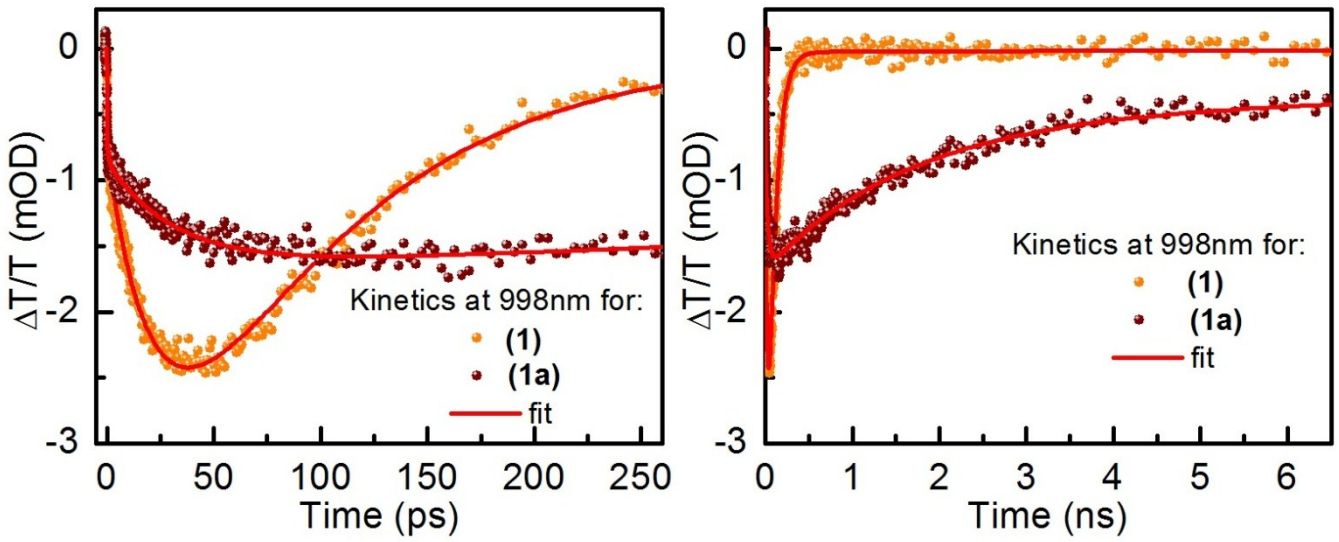

Figure S32. Kinetic traces from TA spectra for **1a** and **1** in benzonitrie at 298 K (λ_{ex} = 525 nm, pulse width ~90 fs): rise (left) and decay (right); monitoring wavelengths is are given on the graph.

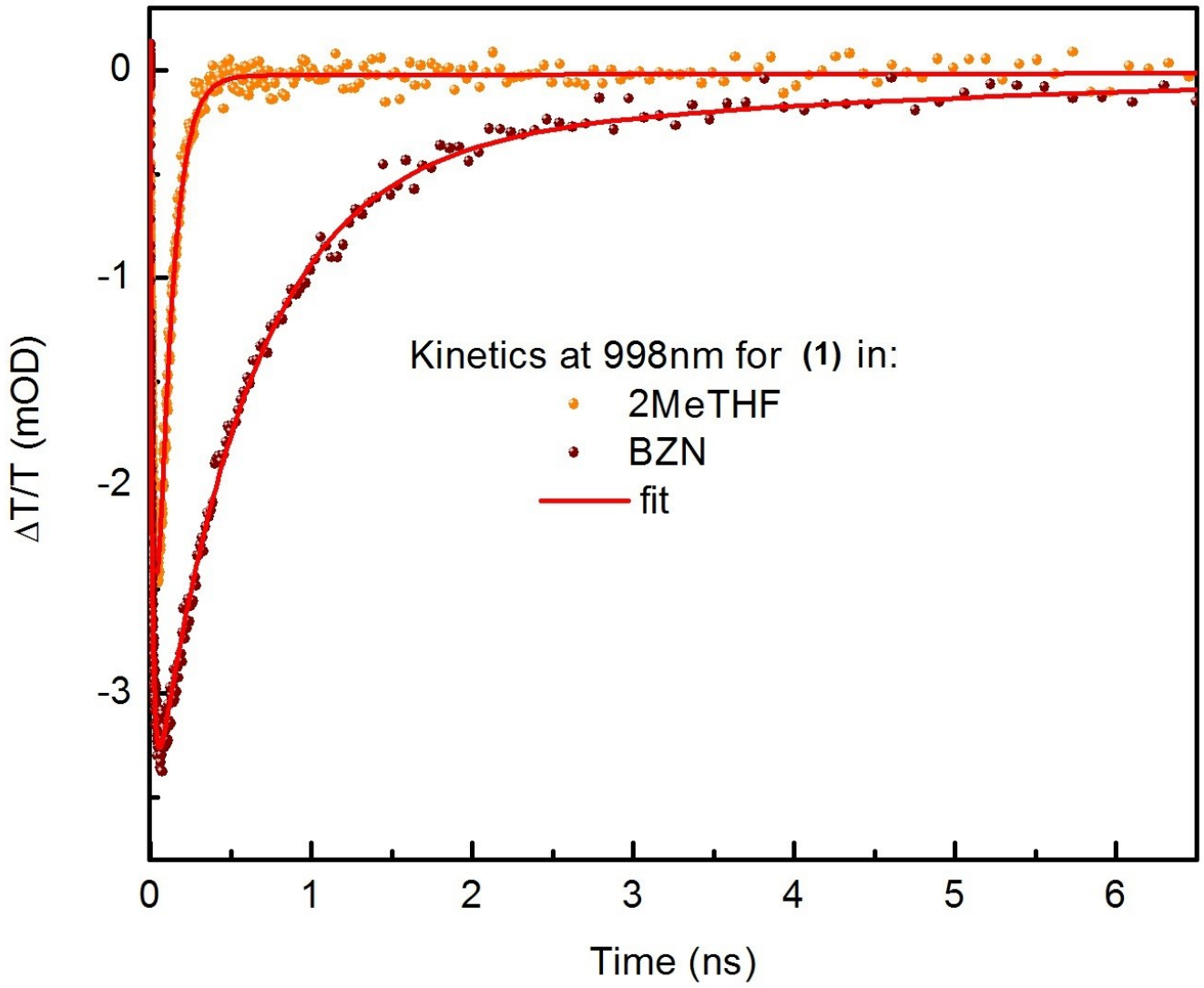

Figure S33. Kinetic traces from TA spectra for **1** in 2MeTHF (brown) and BZN (orange) at 298 K (λ_{ex} = 525 nm, pulse width ~90 fs). The monitoring wavelength are given on graph and the red line show the best fitted kinetic traces.

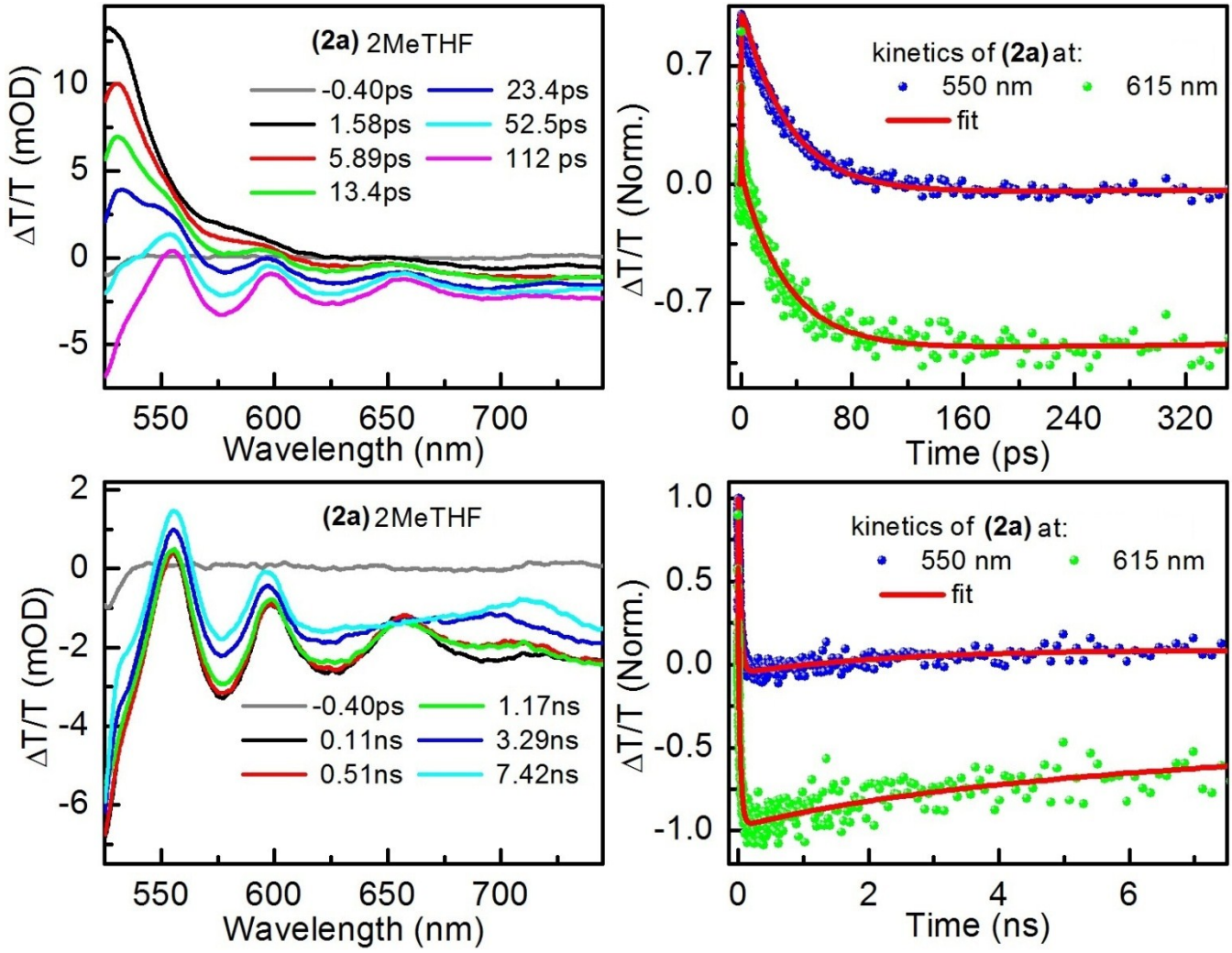

Figure S34. TA spectra (left) and kinetic traces (right) collected for **2a** in 2MeTHF at 298 K (λ_{ex} = 525 nm, pulse width ~90 fs). Delay times for the TA spectra and the monitoring wavelengths for kinetic profile are given on graph and the red lines show the best fitted kinetic traces.

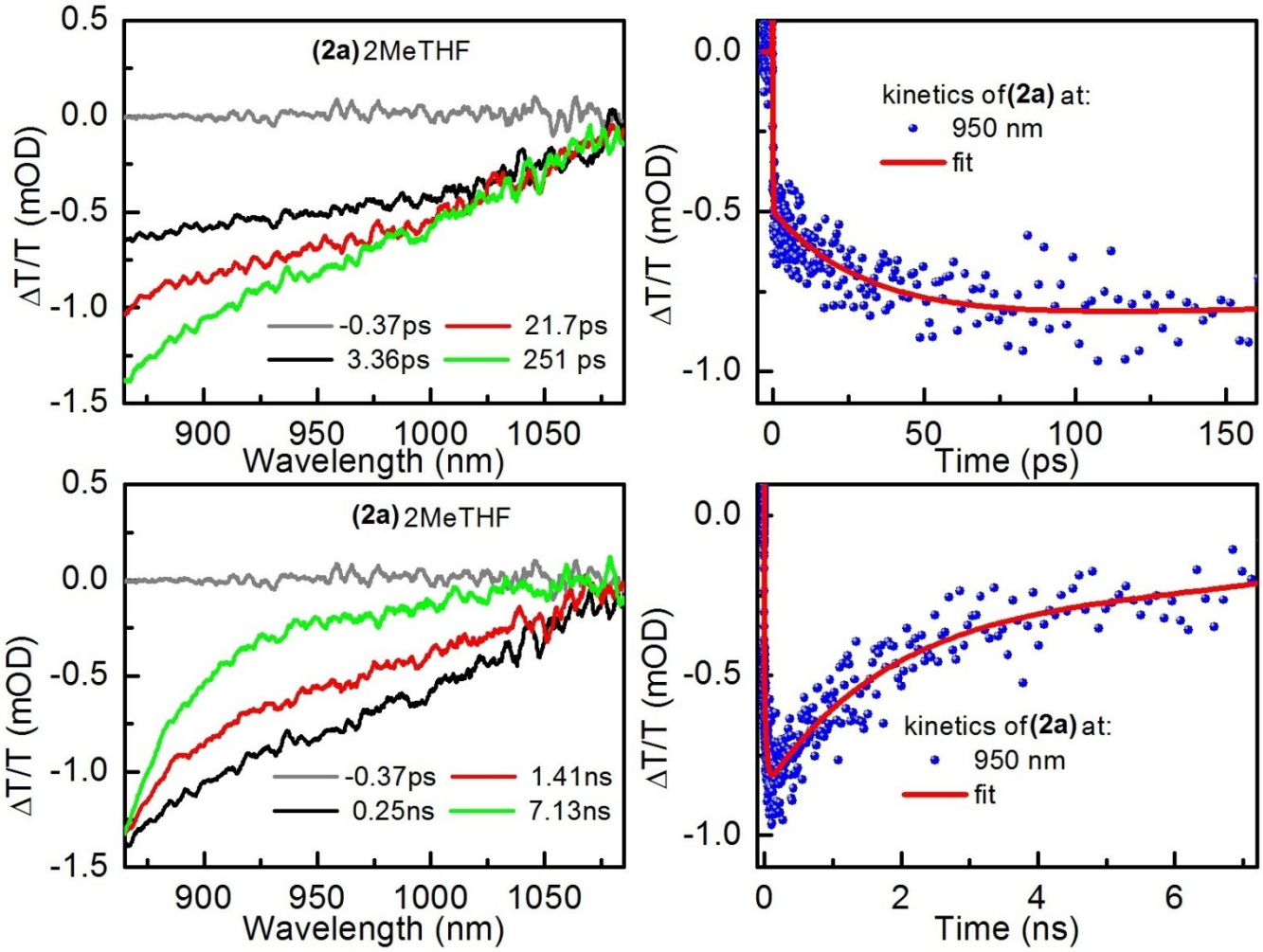

Figure S35. TA spectra (left) and kinetic traces (right) collected for **2a** in 2MeTHF at 298 K (λ_{ex} = 525 nm, pulse width ~90 fs). Delay times for the TA spectra and the monitoring wavelengths for kinetic profile are given on the graph and the red lines show the best fitted kinetic traces.

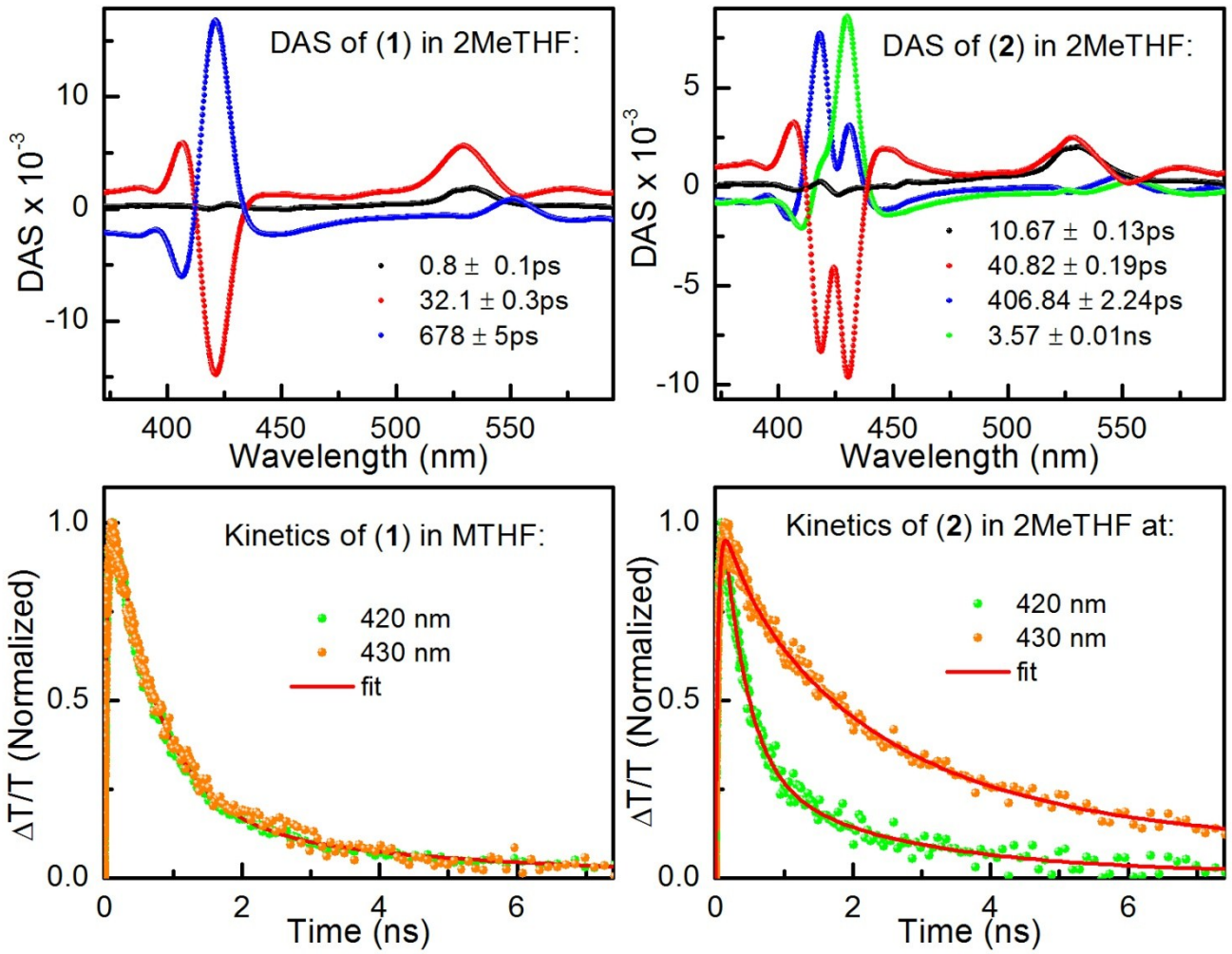

Figure S36. Comparison of decay associated spectra (up) and kinetic profile (down) for (**1**, left) and (**2**, right) in 2MeTHF, (λ_{ex} = 525 nm, laser pulse = 90 fs).

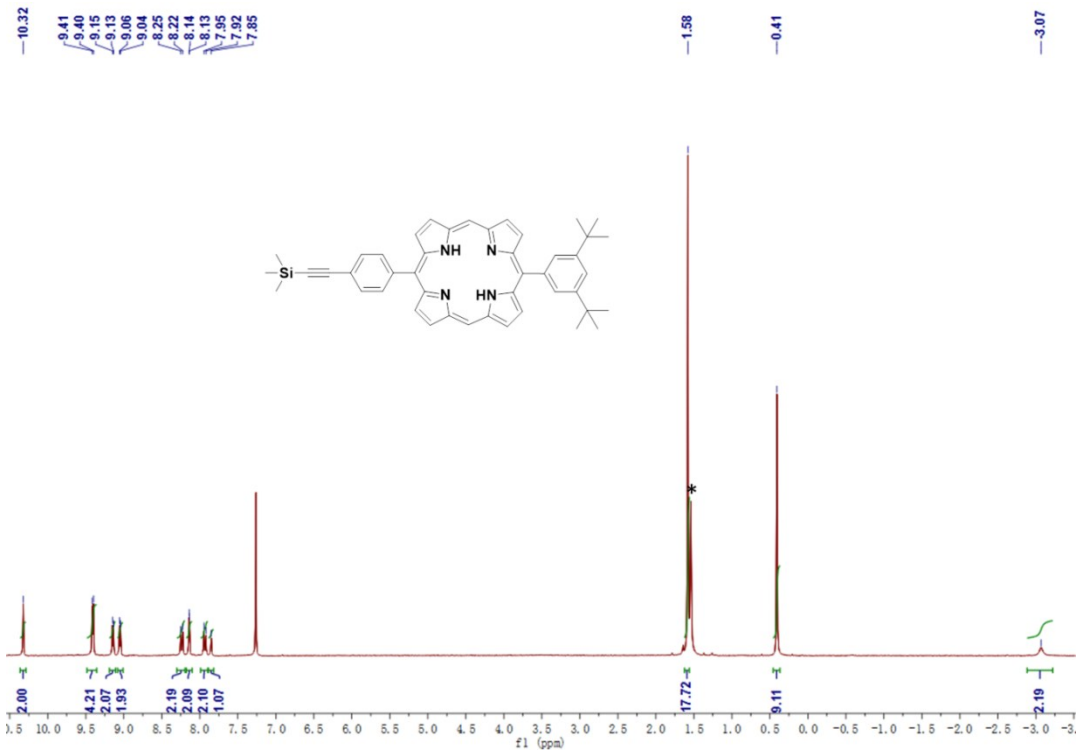

Figure S37. ^{1}H NMR spectra of **1e** in $CDCl_3$.

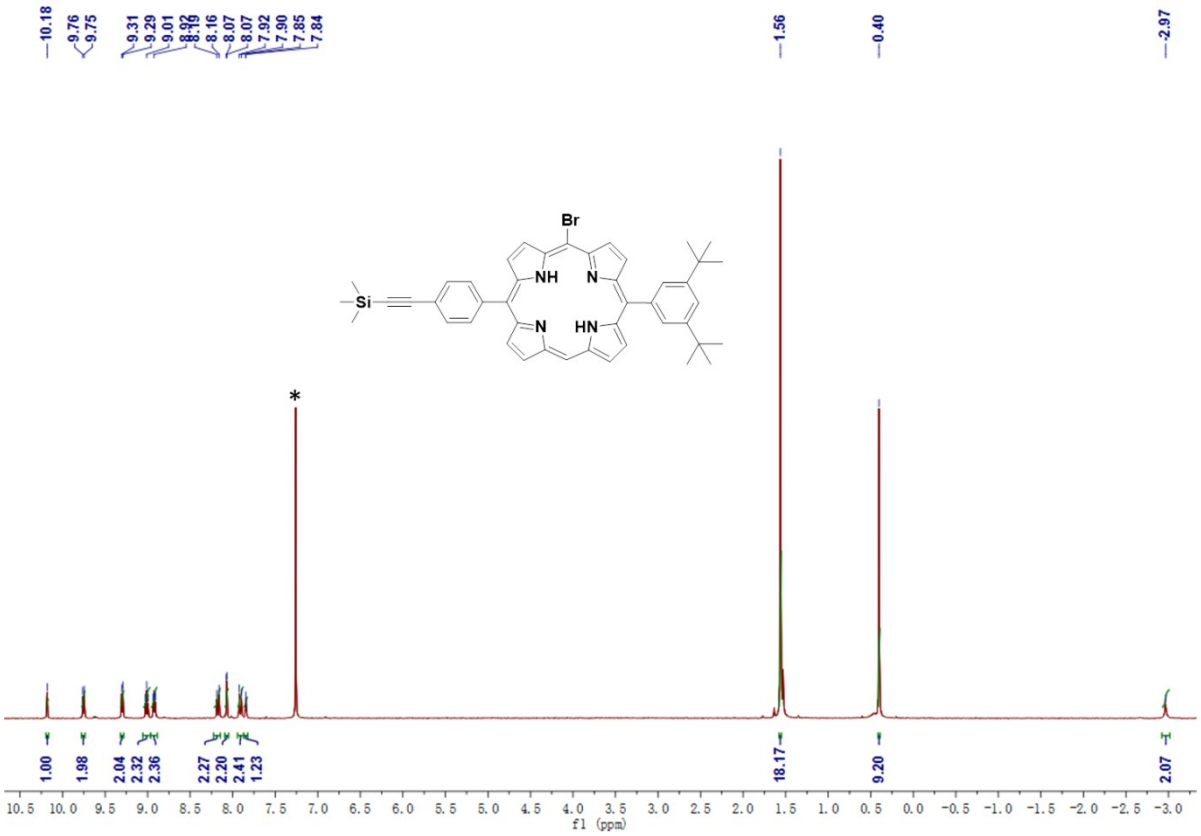

Figure S38. ^{1}H NMR spectra of **1e**-Br in $CDCl_3$.

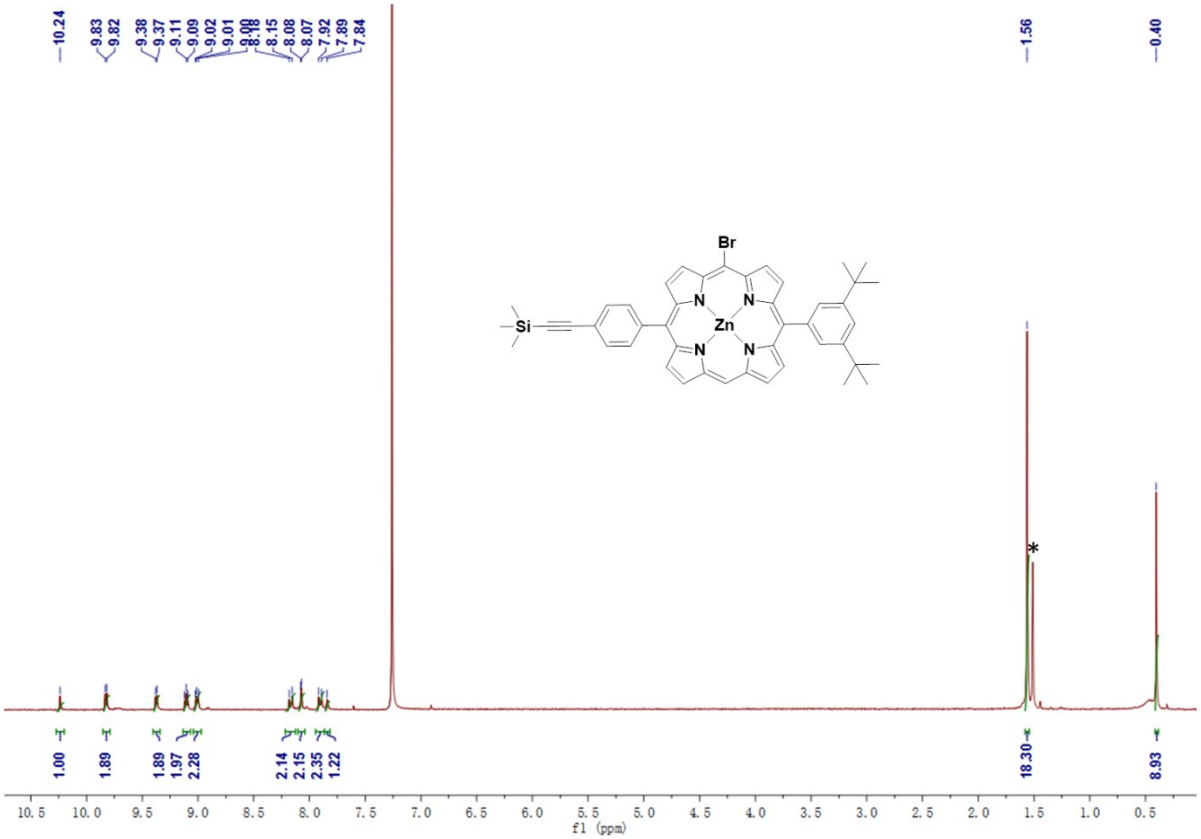

Figure S39. ^{1}H NMR spectra of **1e**-ZnBr in $CDCl_3$.

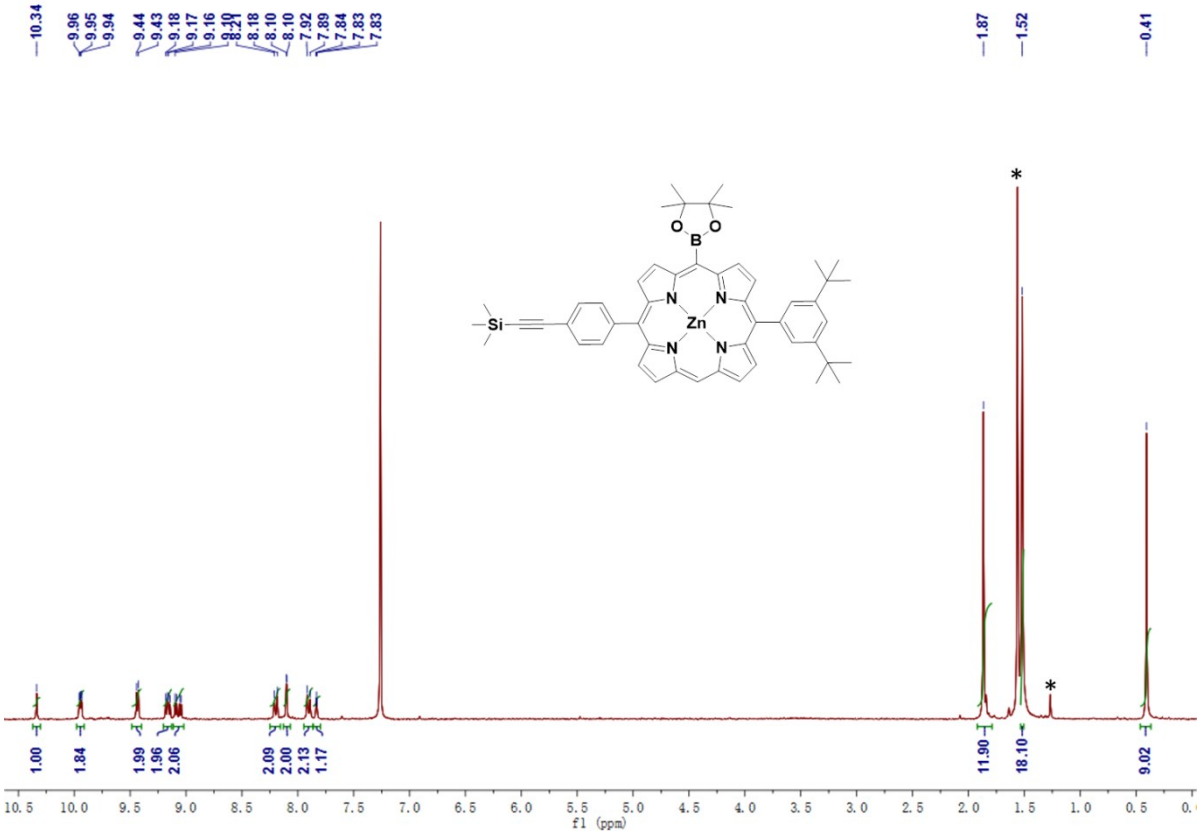

Figure S40. ^{1}H NMR spectra of **1d** in $CDCl_3$.

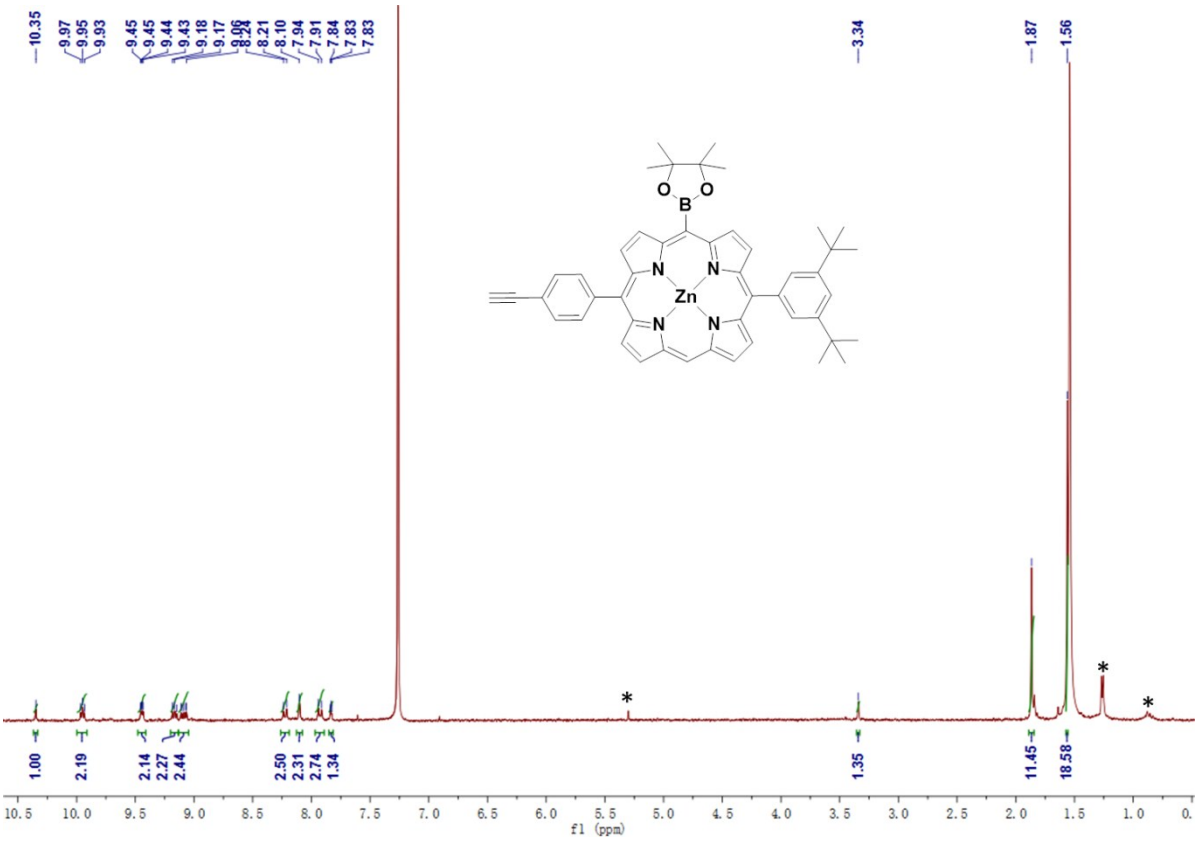

Figure S41. ^{1}H NMR spectra of **1c** in $CDCl_3$.

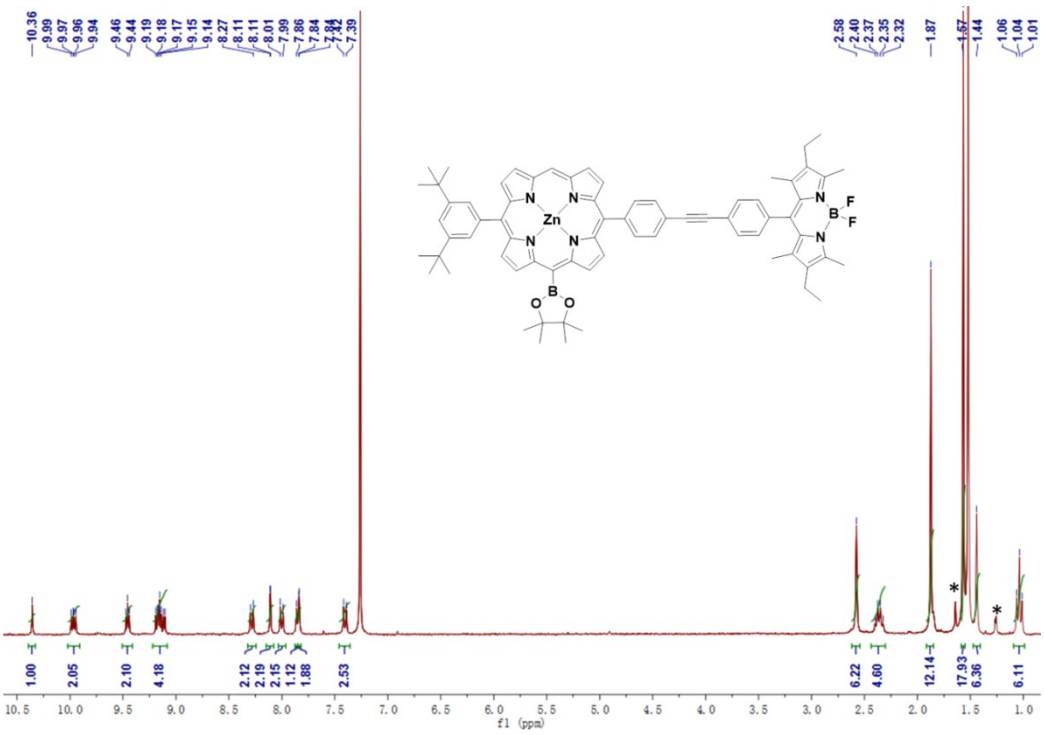

Figure S42. ^{1}H NMR spectra of **1b** in $CDCl_3$.

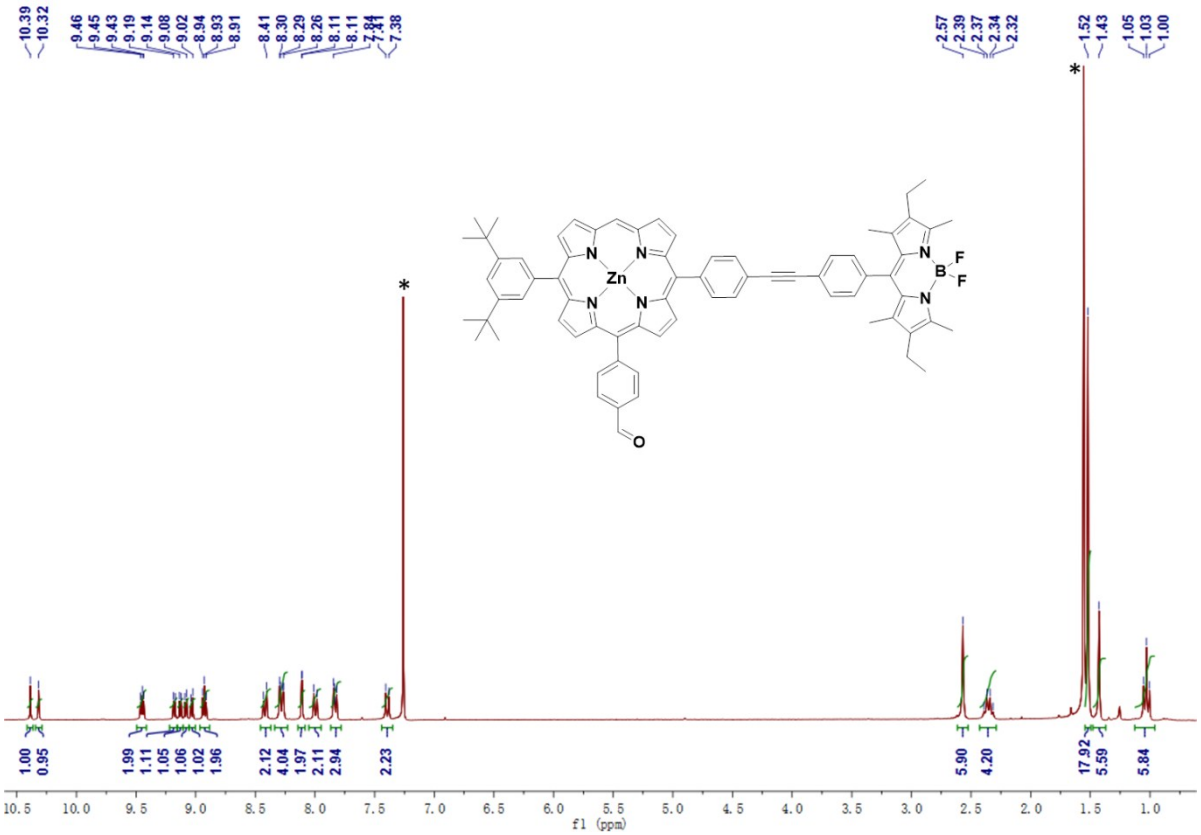

Figure S43. ^{1}H NMR spectra of **1a** in $CDCl_3$.

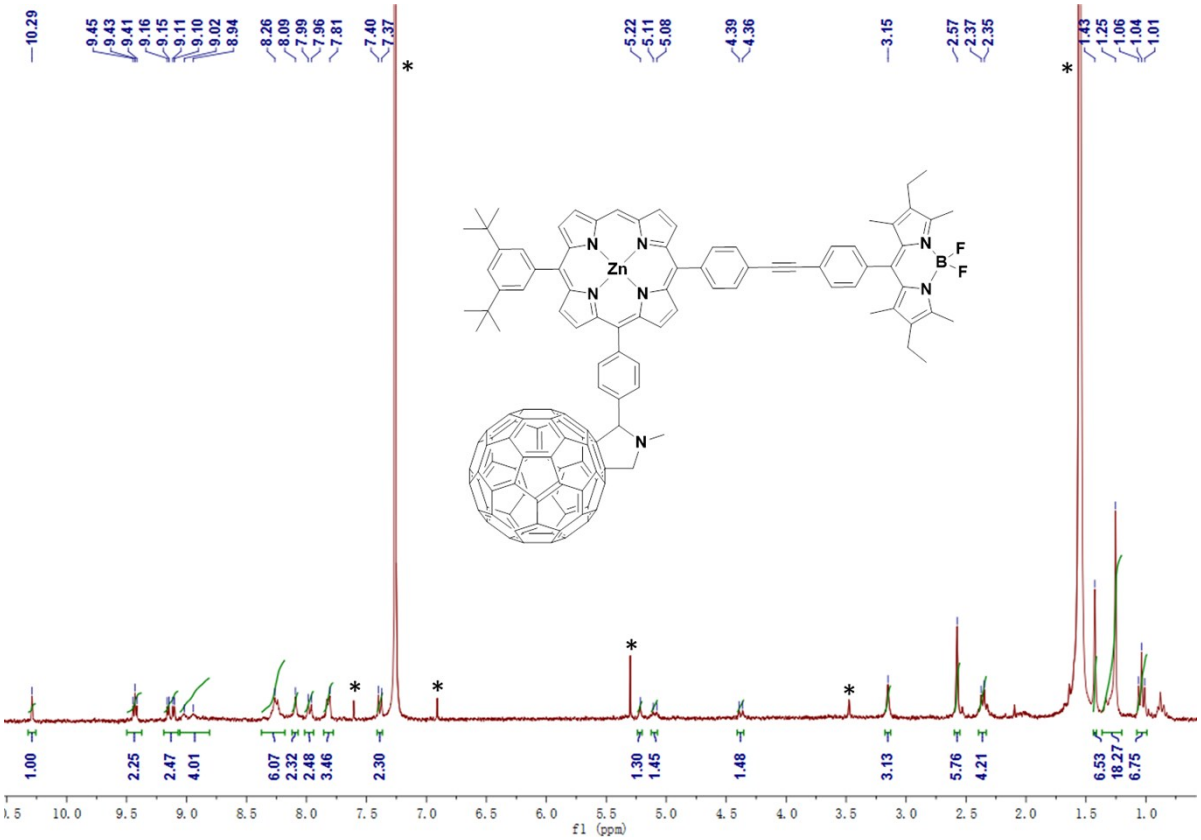

Figure S44. ^{1}H NMR spectra of **1** in $CDCl_3$.

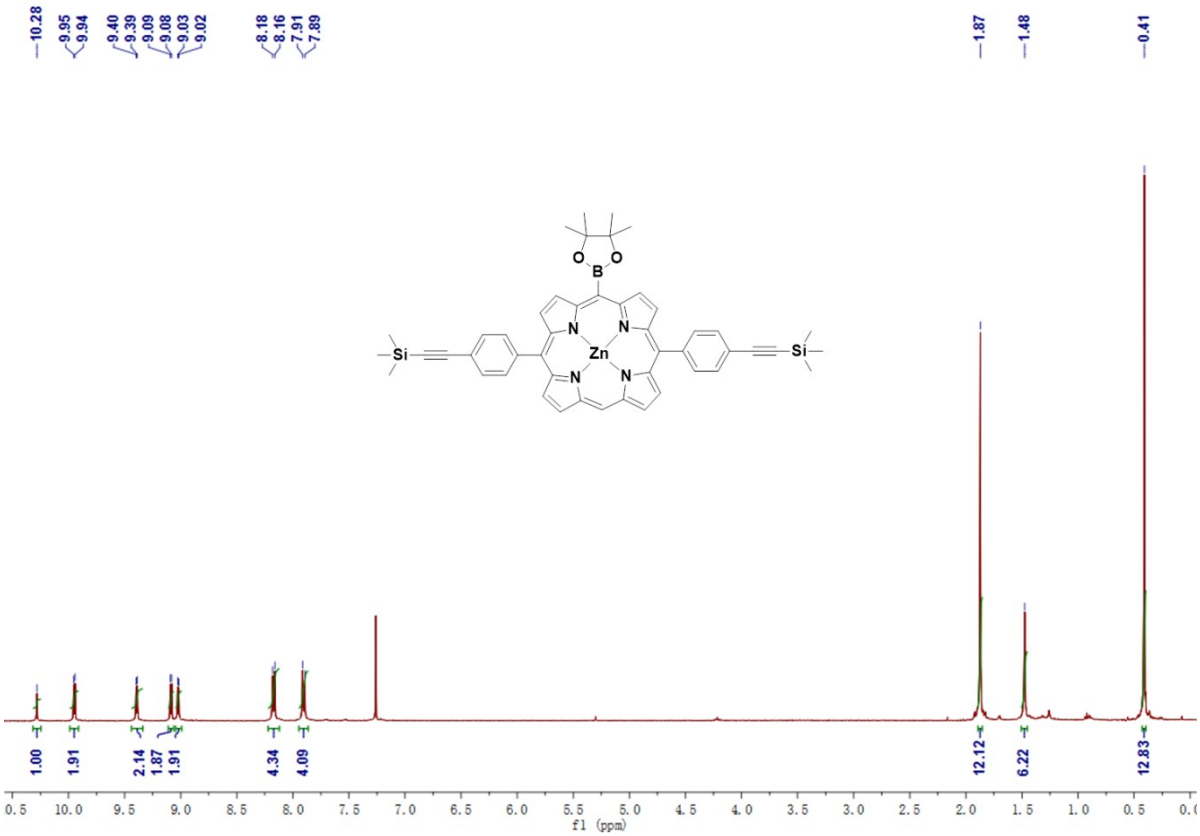

Figure S45. ^{1}H NMR spectra of **2d** in $CDCl_3$.

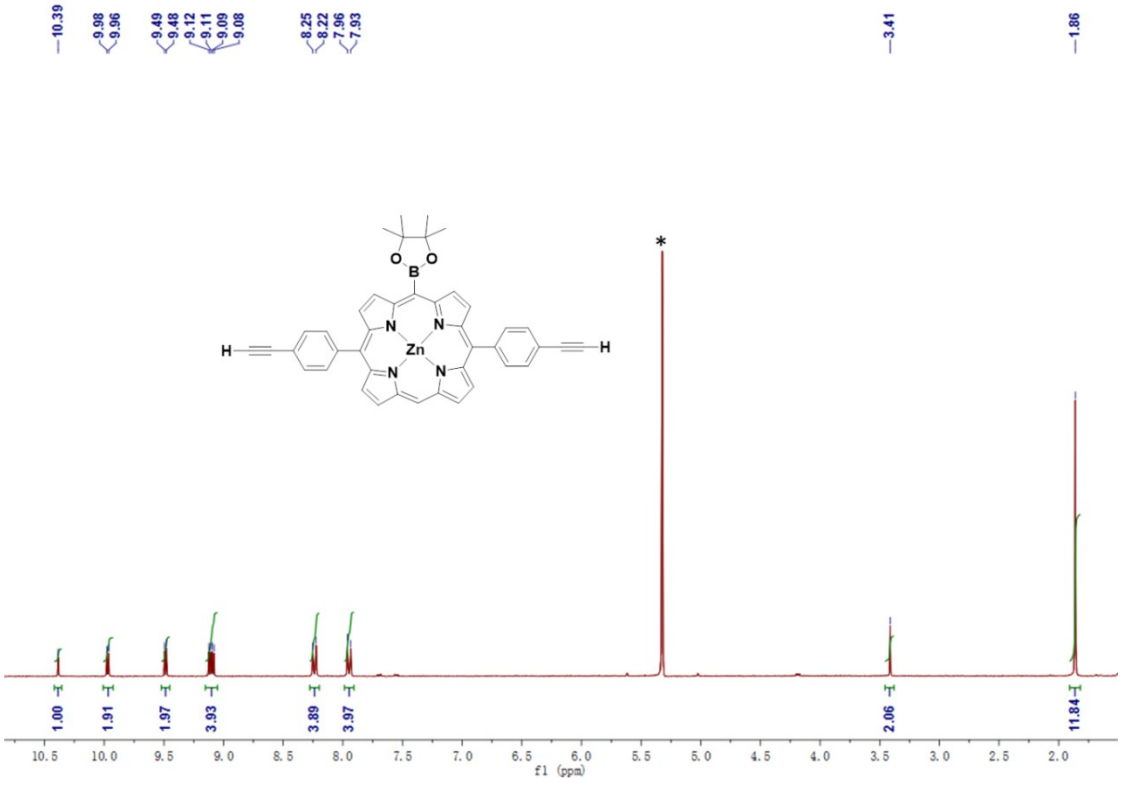

Figure S46. ^{1}H NMR spectra of **2c** in CD_2Cl_2.

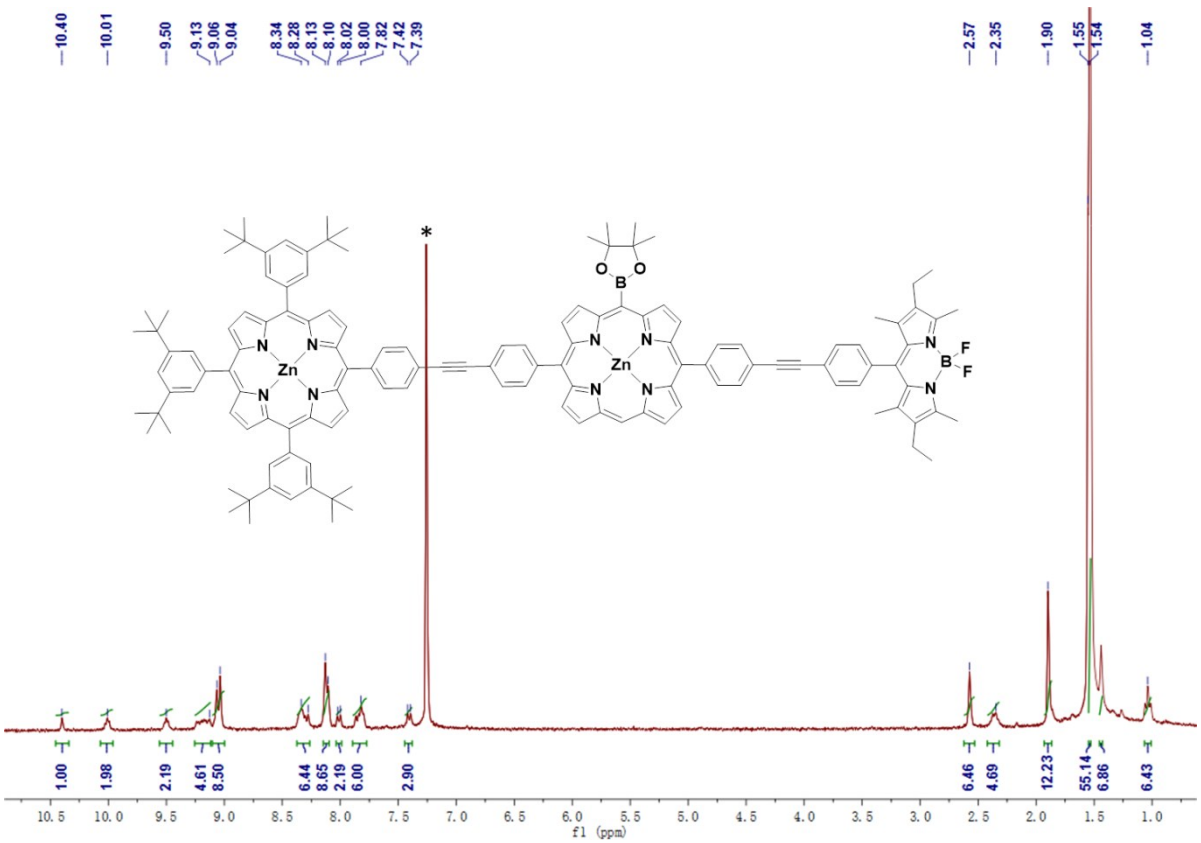

Figure S47. ^{1}H NMR spectra of **2b** in $CDCl_3$.

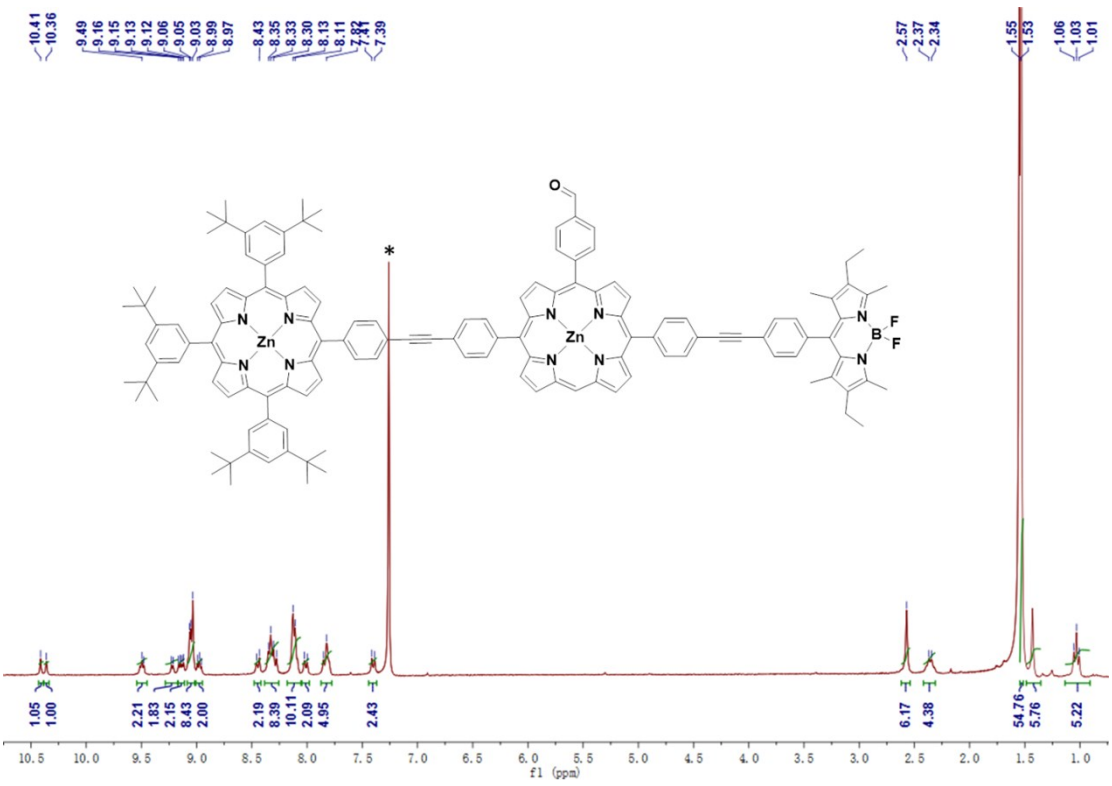

Figure S48. ^{1}H NMR spectra of **2a** in $CDCl_3$.

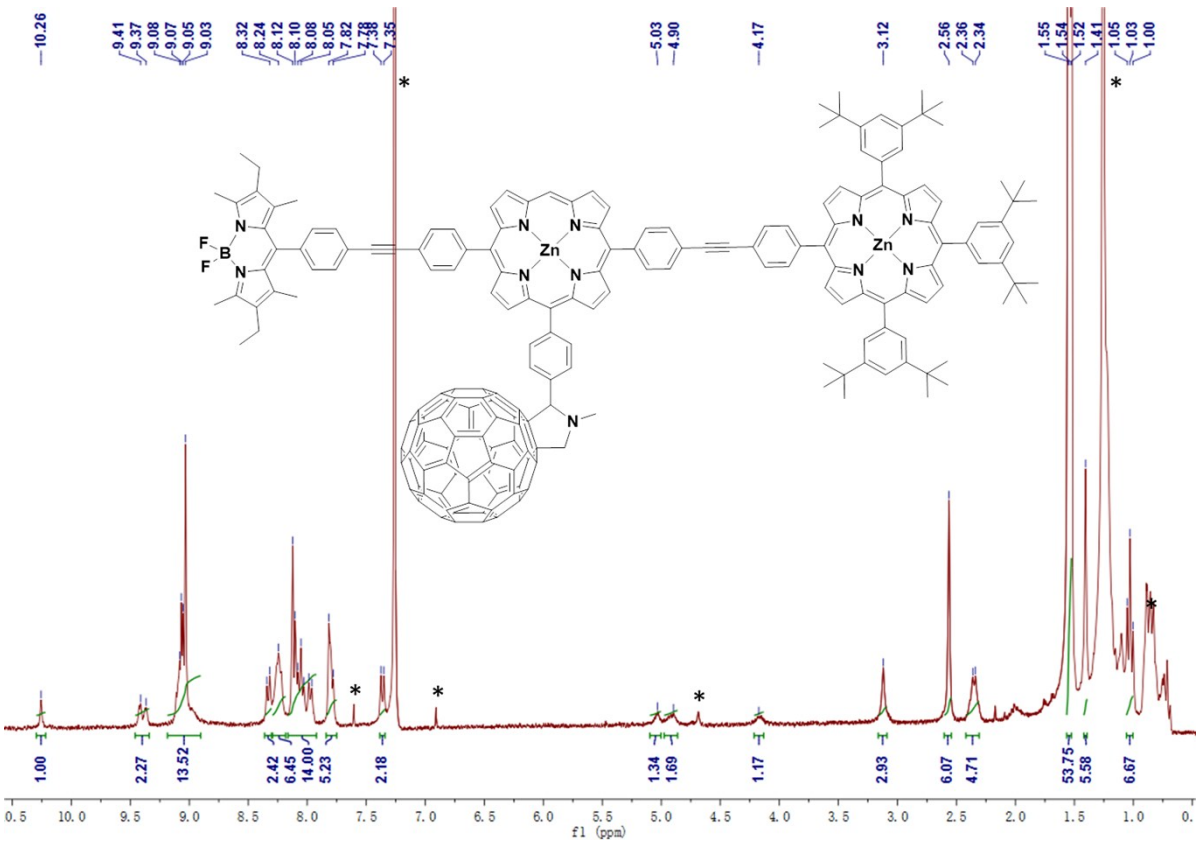

Figure S49. ^{1}H NMR spectra of **2** in $CDCl_3$.

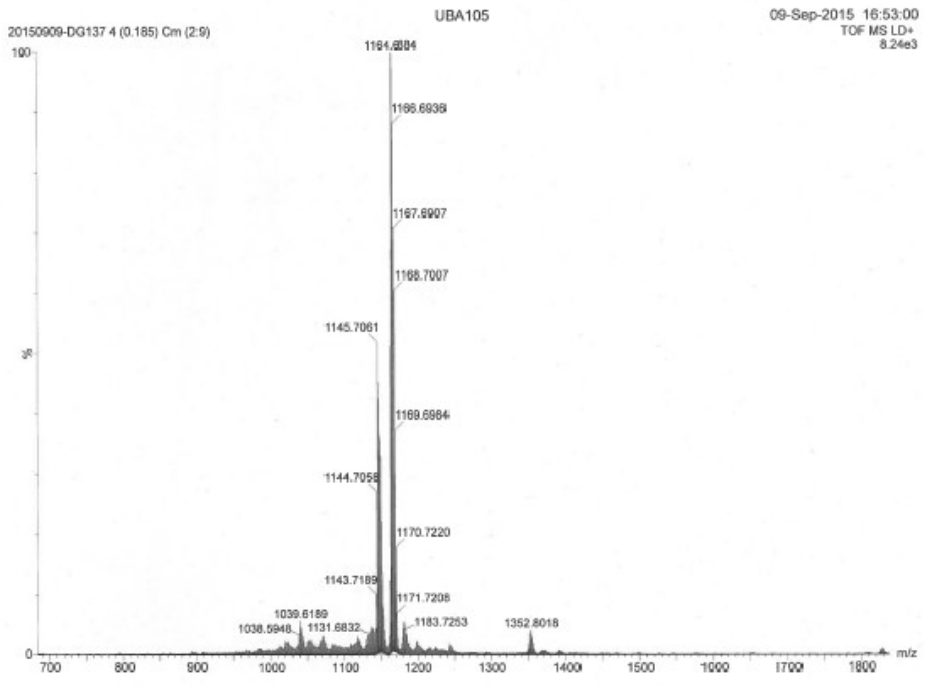

Figure S50. MALDI-TOF spectra of **1b**.

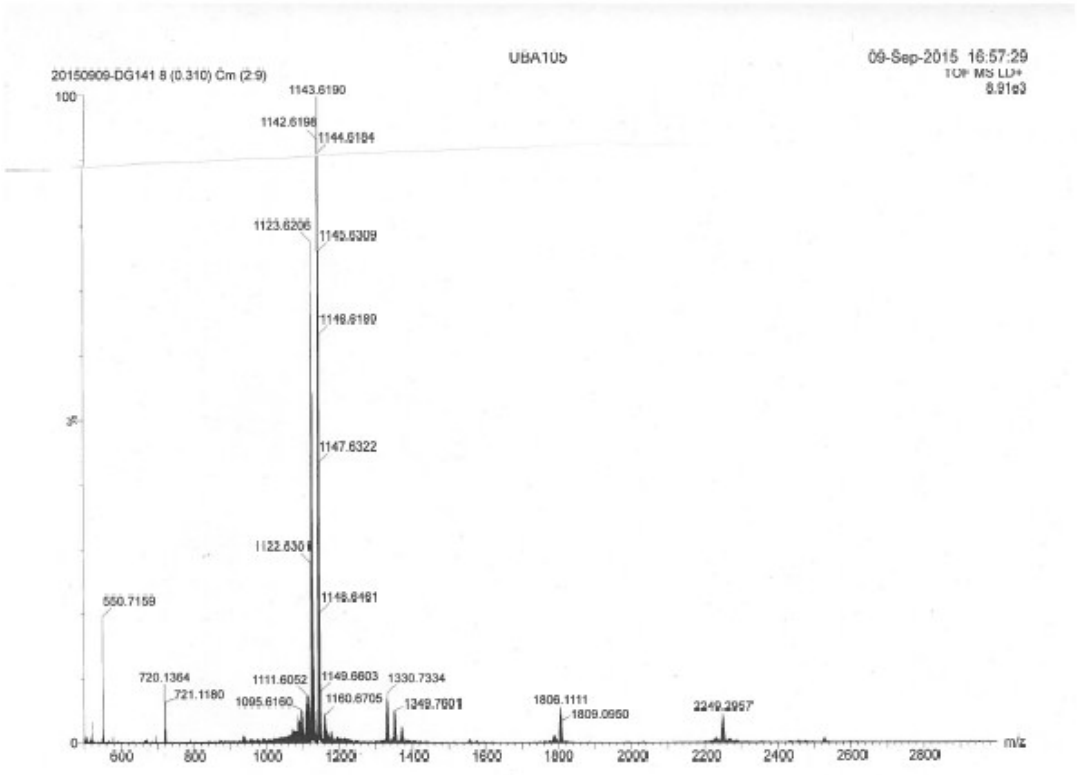

Figure S51. MALDI-TOF spectra of **1a**.

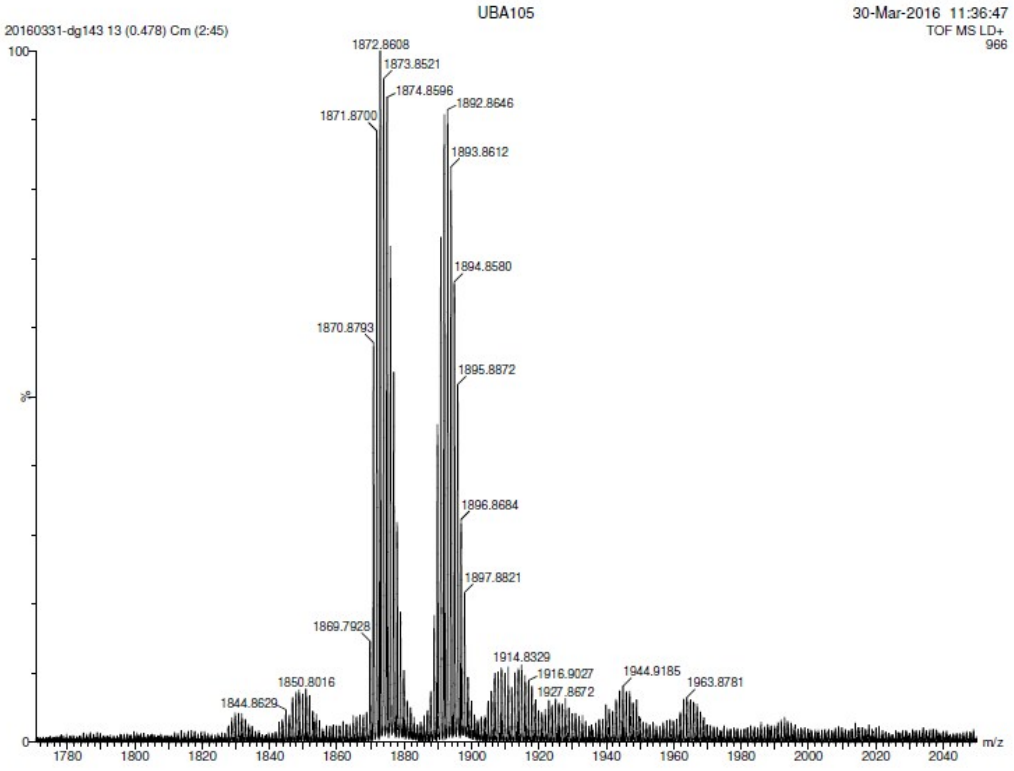

Figure S52. MALDI-TOF spectra of **1**.

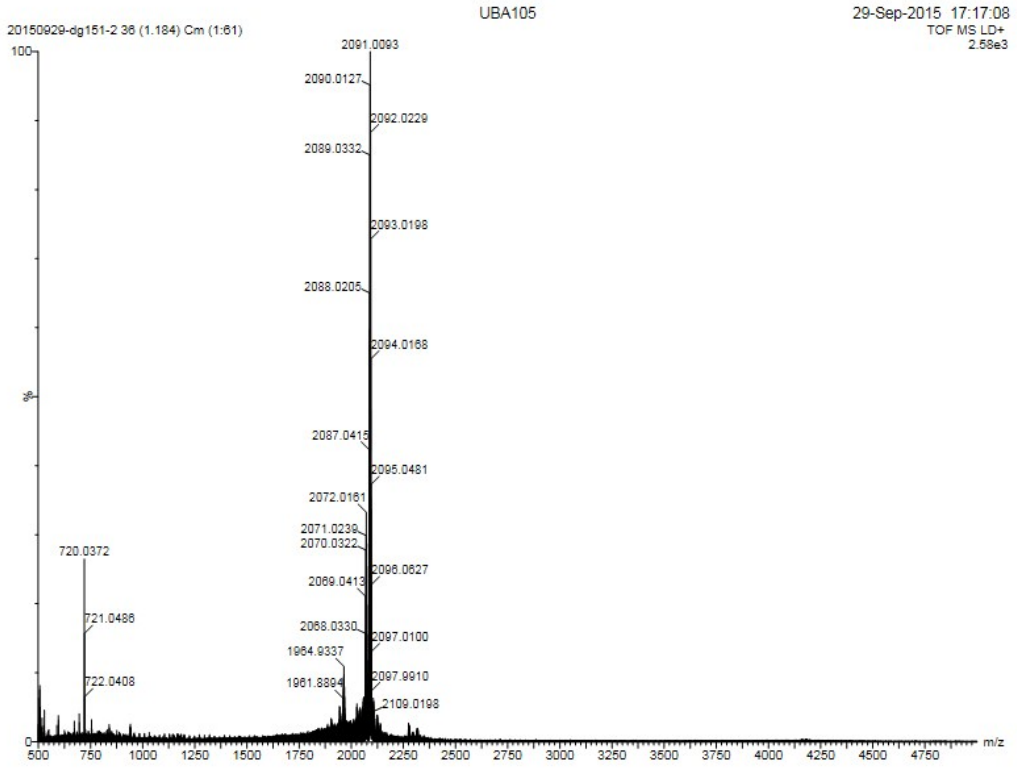

Figure S53. MALDI-TOF spectra of **2b**.

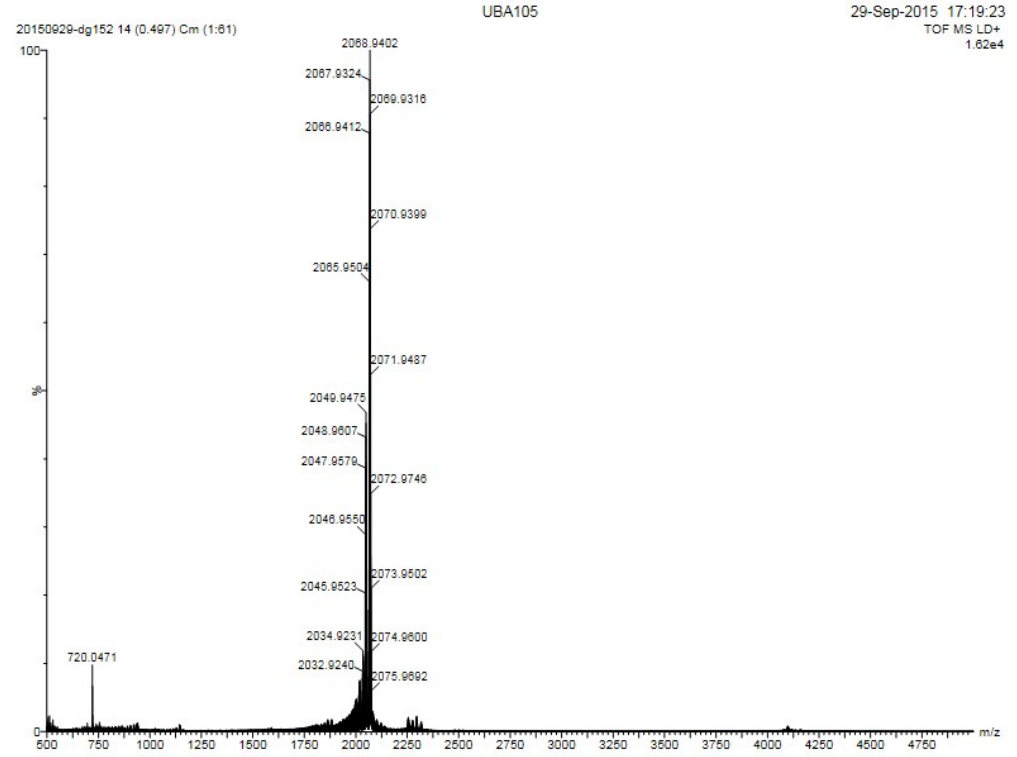

Figure S54. MALDI-TOF spectra of **2a**.

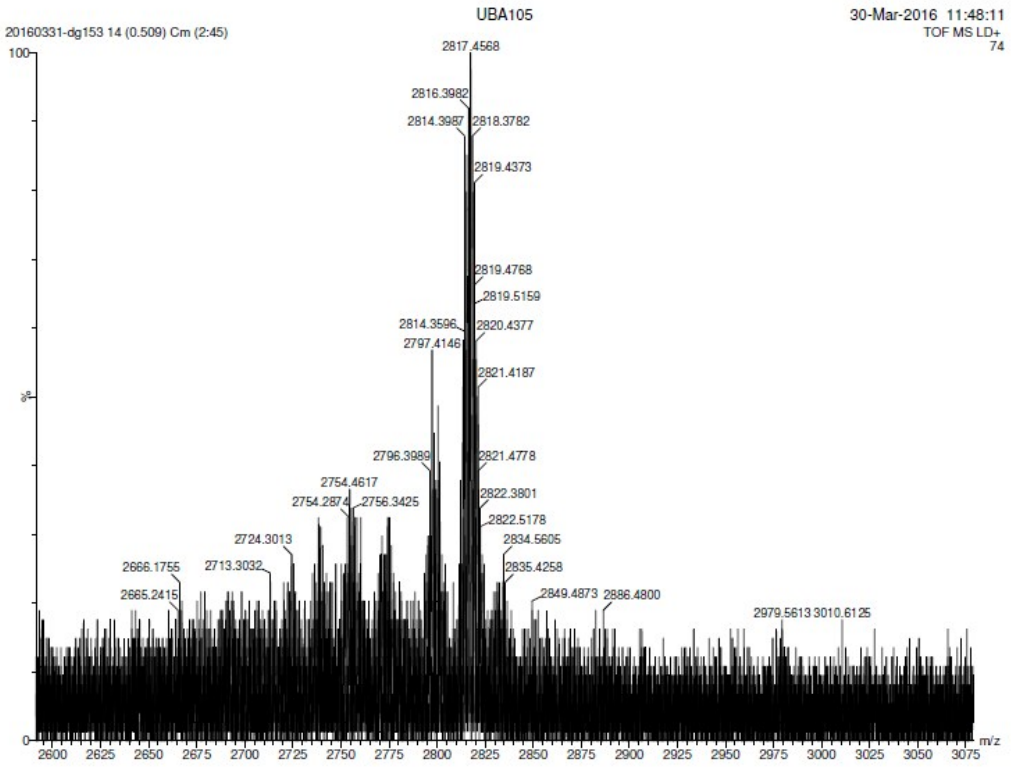

Figure S55. MALDI-TOF spectra of **2**.

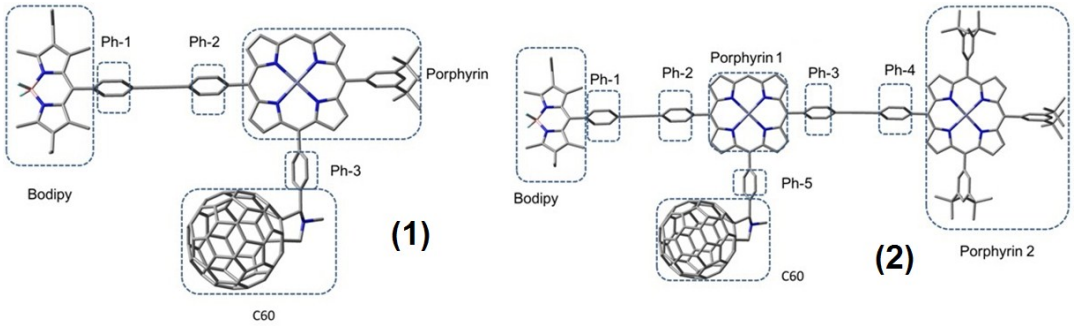

* H = HOMO, L=LUMO, Por = porphyrin, C_{60} = fullerene, and Ph = Benzene

Table S1**:** Quantitative atomic contributions for each fragments building **1** and **2**.

		MOs									
		H-4	H-3	H-2	H-1	H	L	L+1	L+2	L+3	L+4
1	BODIPY	0	**99.73**	0	0	0.12	0	0	0	**92.0**	0.82
	Por	0.12	0	**96.7**	0.48	**87.3**	1.44	0.19	0.42	0.47	**89.3**
	C_{60}	**99.2**	0	0.37	**99.2**	0.78	**99.3**	**99.5**	**99.4**	0	0.24
	Ph-1	0.01	0.27	0	0	1.41	0	0	0	7.3	1.56
	Ph-2	0.02	0	1.48	0.02	5.69	0	0	0	0.22	6.14
	Ph-3	0.66	0	1.41	0.33	4.67	0.54	0.34	0.16	0	1.93

		MOs											
		H-4	H-3	H-2	H-1	H	L	L+1	L+2	L+3	L+4	L+5	L+6
2	BODIPY	**99.8**	0	0	0.12	0	0	0	0	**92.89**	0.16	0	0.01
	Por 1	0	0	0.5	**76.6**	3.16	0.14	0.19	0.43	0	**79.8**	**85.6**	4.64
	Por 2	0	**98.5**	0.01	4.9	**88.9**	0	0	0	0	4.31	0.03	**88.3**
	C_{60}	0	0	**99.1**	1.00	0.02	**99.3**	**99.5**	**99.4**	0	0.06	5.44	0.08
	Ph-1	0.2	0	0	1.48	0.05	0	0	0	7.09	1.37	0	0.1
	Ph-2	0	0	0.03	5.60	0.2	0	0	0	0.02	5.61	2.25	0.36
	Ph-3	0	0	0.03	4.94	1.88	0	0	0	0	5.45	2.080	1.07
	Ph-4	0	1.48	0	1.12	5.58	0	0	0	0	1.60	0	5.3
	Ph-5	0	0	0.03	4.28	0.16	0.54	0.35	0.16	0	1.68	4.56	0.04

Table S2**:** Calculated position, oscillator strength (f) and major contributions of the first 100 singlet-singlet electronic transitions for **1**.

No.	Wavelength (nm)	Osc. Strength	Major contribs (%)
1	992.8	0.0049	H-3→LUMO (97)
2	878.8	0.0027	HOMO→LUMO (99)
3	789.0	0	H-2→LUMO (99)
4	779.6	0	H-1→LUMO (100)
5	760.2	0.0013	H-3→L+1 (94)
6	707.8	0.0015	H-6→LUMO (22), H-4→LUMO (71)
7	698.8	0.0011	H-5→LUMO (91)
8	697.1	0	HOMO→L+1 (99)
9	687.0	0.0005	H-6→LUMO (70), H-4→LUMO (24)
10	664.6	0.0032	H-3→L+2 (91)
11	639.6	0	H-2→L+1 (98)
12	639.0	0	H-1→L+1 (100)
13	619.6	0.0002	HOMO→L+2 (99)
14	605.6	0	H-4→L+1 (93)
15	579.7	0.0003	H-5→L+1 (80)
16	575.6	0.0003	H-6→L+1 (91)
17	575.5	0	H-1→L+2 (100)
18	573.7	0.0002	H-2→L+2 (98)
19	561.3	0.0038	H-9→LUMO (89)
20	549.7	0.0002	H-7→LUMO (99)
21	537.8	0.0006	H-5→L+2 (84), H-4→L+2 (12)
22	535.3	0.0509	H-2→L+6 (37), HOMO→L+5 (53)
23	534.3	0.0071	H-2→L+5 (33), HOMO→L+6 (46)
24	533.6	0.0008	H-5→L+2 (10), H-4→L+2 (62)
25	509.9	0.0018	H-6→L+2 (79)
26	507.8	0.0091	H-11→LUMO (18), H-3→L+3 (75)
27	507.1	0.0015	H-11→LUMO (75), H-3→L+3 (18)
28	482.8	0.0018	HOMO→L+3 (96)
29	481.5	0	H-8→LUMO (99)
30	480.9	0.0022	H-9→L+1 (86)
31	475.7	0	H-7→L+1 (97)
32	472.8	0.0017	H-18→LUMO (94)
33	470.8	0.0056	HOMO→L+4 (90)
34	457.1	0	H-1→L+3 (100)
35	455.4	0.0008	H-9→L+2 (85)
36	454.4	0.0008	H-2→L+3 (90)
37	451.3	0.0046	H-1→L+4 (16), H-1→L+5 (82)
38	447.9	0	H-10→LUMO (99)
39	445.1	0.0052	H-15→LUMO (29), H-12→LUMO (53)
40	443.2	0.0006	H-3→L+4 (16), H-3→L+5 (67)

41	442.9	0	H-1→L+6 (100)
42	442.0	0.0008	H-3→L+7 (14), H-2→L+4 (74)
43	442.0	0.0018	H-5→L+3 (11), H-3→L+7 (50), H-2→L+4 (16)
44	440.2	0.0017	H-3→L+6 (85)
45	439.5	0.0066	H-19→LUMO (19), H-16→LUMO (22), H-13→LUMO (40)
46	438.9	0.0006	H-7→L+2 (92)
47	436.3	0.0029	H-19→LUMO (10), H-14→LUMO (37), H-13→LUMO (31), H-12→LUMO (14)
48	433.4	0.001	H-14→LUMO (55), H-12→LUMO (22)
49	433.3	0.0001	H-3→L+4 (80), H-3→L+5 (19)
50	431.9	0.4168	H-8→L+4 (12), H-1→L+4 (72), H-1→L+5 (16)
51	430.7	0.0037	H-19→LUMO (11), H-15→LUMO (55), H-13→LUMO (10)
52	429.8	0.0037	H-6→L+3 (29), H-4→L+3 (50)
53	427.0	0.0045	H-6→L+3 (56), H-4→L+3 (28)
54	426.5	0.0005	H-11→L+1 (96)
55	424.0	0	H-8→L+1 (99)
56	422.4	0.0062	H-5→L+3 (67), H-3→L+7 (10), H-3→L+8 (11)
57	420.5	0.0014	H-19→LUMO (32), H-16→LUMO (45)
58	418.2	0.0007	HOMO→L+7 (91)
59	417.2	0.0027	H-20→LUMO (19), H-18→L+1 (25), H-3→L+8 (20)
60	415.3	0.0086	H-18→L+1 (17), H-17→LUMO (51), H-3→L+8 (14)
61	414.9	0.0117	H-18→L+1 (33), H-17→LUMO (38)
62	407.7	0.0032	H-25→LUMO (15), H-20→LUMO (42), H-3→L+8 (10)
63	404.3	0.0047	H-29→LUMO (10), H-23→LUMO (11), H-22→LUMO (48)
64	401.6	1.6312	H-2→L+6 (29), HOMO→L+5 (21), HOMO→L+9 (32)
65	400.3	0.0402	H-24→LUMO (47), H-11→L+2 (17)
66	399.7	0.0034	H-24→LUMO (12), H-11→L+2 (78)
67	397.8	0.0105	H-28→LUMO (15), H-26→LUMO (28), H-25→LUMO (11), H-20→LUMO (11)
68	397.6	0	H-10→L+1 (99)
69	396.8	0.0023	H-2→L+7 (97)
70	396.6	0	H-1→L+7 (100)
71	395.1	0	H-8→L+2 (99)
72	393.7	0.0059	HOMO->L+8 (91)
73	393.2	0.0065	H-29→LUMO (18), H-28→LUMO (15), H-27→LUMO (13), H-26→LUMO (11)
74	392.5	0	H-15→L+1 (27), H-12→L+1 (53)
75	392.2	0.0003	H-7→L+4 (87)
76	391.9	0.0024	H-18→L+2 (52)
77	389.0	0.0075	H-28→LUMO (23), H-25→LUMO (37)
78	387.6	0.0284	H-27→LUMO (32), H-13→L+1 (31)
79	387.4	0.0005	H-1→L+9 (93)
80	387.2	0.1559	H-27→LUMO (19), H-13→L+1 (43)
81	386.3	0.5466	H-2→L+5 (30), HOMO→L+6 (23)
82	385.3	0.0107	H-14→L+1 (69)

83	383.6	0.0004	H-16→L+1 (11), H-15→L+1 (29), H-14→L+1 (20), H-12→L+1 (26)
84	383.3	0.0994	H-7→L+5 (41), HOMO→L+9 (34)
85	383.1	0.0353	H-29→LUMO (13), H-22→L+1 (10)
86	380.7	0.0004	H-19→L+1 (22), H-16→L+1 (30), H-15→L+1 (22)
87	380.1	0.0016	H-4→L+4 (21), H-4→L+5 (68)
88	377.6	0.0036	H-4→L+6 (73)
89	377.5	0.0006	H-25→LUMO (12), H-5→L+7 (41), H-4→L+6 (13)
90	376.3	0.0045	H-4→L+7 (48)
91	375.6	0.0002	H-21→LUMO (95)
92	374.9	0.0004	H-5→L+4 (20), H-5→L+5 (63), H-4→L+4 (11)
93	374.5	0.2013	H-8→L+4 (75), H-1→L+4 (13)
94	374.5	0.0012	H-4→L+4 (13), H-2→L+8 (78)
95	374.4	0.0025	H-4→L+4 (52), H-4→L+5 (20), H-2→L+8 (18)
96	372.6	0.0011	H-19→L+1 (32), H-17→L+1 (14), H-16→L+1 (27)
97	372.5	0.0001	H-1→L+8 (98)
98	372.3	0.0011	H-5→L+6 (86)
99	372.1	0	H-10→L+2 (98)
100	371.5	0.028	H-7→L+6 (48), H-2→L+9 (23)

Table S3**:** Calculated position, oscillator strength (f) and major contributions of the first 100 singlet-singlet electronic transitions for **2**.

No.	Wavelength (nm)	Osc. Strength	Major contribs (%)
1	992.6	0.0048	H-5→LUMO (13), H-4→LUMO (86)
2	913.0	0.0002	HOMO→LUMO (98)
3	850.8	0.0025	H-2→LUMO (97)
4	796.9	0	H-1→LUMO (100)
5	780.8	0	H-3→LUMO (100)
6	763.3	0	H-5→LUMO (85), H-4→LUMO (12)
7	760.2	0.0013	H-5→L+1 (12), H-4→L+1 (81)
8	720.5	0	HOMO→L+1 (98)
9	707.5	0.0015	H-9→LUMO (23), H-6→LUMO (70)
10	698.4	0.0011	H-8→LUMO (91)
11	686.9	0.0005	H-9→LUMO (70), H-6→LUMO (24)
12	679.9	0	H-2→L+1 (97)
13	664.5	0.0034	H-5→L+2 (12), H-4→L+2 (79)
14	646.3	0	H-1→L+1 (100)
15	640.1	0	H-3→L+1 (100)
16	639.1	0	HOMO→L+2 (98)
17	622.8	0	H-5→L+1 (87), H-4→L+1 (12)
18	606.0	0.0002	H-6→L+1 (10), H-2→L+2 (87)
19	605.3	0.0001	H-6→L+1 (82), H-2→L+2 (11)
20	580.1	0	H-1→L+2 (100)
21	579.6	0.0004	H-8→L+1 (81)
22	576.4	0	H-3→L+2 (100)
23	575.6	0.0003	H-9→L+1 (90)
24	571.8	0	H-7→LUMO (99)
25	561.2	0.0034	H-12→LUMO (82)
26	559.9	0.0011	H-5→L+2 (79), H-4→L+2 (13)
27	544.3	0.2094	H-2→L+3 (11), H-1→L+8 (28), HOMO→L+7 (46)
28	542.5	0.0004	H-10→LUMO (98)
29	540.7	0.0163	H-1→L+7 (40), HOMO→L+8 (58)
30	538.8	0.0544	H-5→L+6 (21), H-2→L+3 (48), HOMO→L+7 (12)
31	537.6	0.001	H-8→L+2 (82), H-6→L+2 (12)
32	536.6	0.0046	H-5→L+3 (35), H-2→L+6 (45)
33	533.5	0.0008	H-8→L+2 (13), H-6→L+2 (70)
34	509.9	0.0022	H-9→L+2 (79)
35	509.7	0.0151	HOMO→L+3 (88)
36	507.5	0.0089	H-20→LUMO (16), H-4→L+4 (62)
37	506.9	0.0015	H-20→LUMO (78), H-4→L+4 (13)
38	499.0	0.0002	HOMO→L+4 (54), HOMO→L+6 (43)
39	494.0	0	HOMO→L+4 (44), HOMO→L+6 (54)
40	489.7	0	H-7→L+1 (97)
41	485.2	0	HOMO→L+5 (99)

42	482.0	0	H-11→LUMO (99)
43	480.9	0.0022	H-12→L+1 (87)
44	474.3	0.0017	H-2→L+4 (85), H-2→L+6 (11)
45	472.7	0.0021	H-28→LUMO (91)
46	472.4	0.0014	H-1→L+3 (98)
47	470.1	0	H-10→L+1 (96)
48	463.1	0	H-3→L+3 (99)
49	462.7	0	H-1→L+4 (53), H-1→L+6 (47)
50	462.6	0	H-2→L+5 (98)
51	458.1	0	H-1→L+4 (47), H-1→L+6 (53)
52	457.7	0	H-3→L+4 (99)
53	456.7	0	H-14→LUMO (26), H-13→LUMO (74)
54	455.3	0.0009	H-12→L+2 (91)
55	454.7	0.0003	H-5→L+3 (13), H-4→L+3 (85)
56	453.1	0	H-14→LUMO (74), H-13→LUMO (26)
57	450.7	0	H-1→L+5 (100)
58	450.5	0.0001	H-7→L+2 (97)
59	450.2	0	H-3→L+6 (99)
60	448.1	0	H-16→LUMO (99)
61	447.7	0.0018	H-5→L+6 (12), H-4→L+6 (79)
62	445.6	0.0053	H-5→L+4 (77), H-4→L+4 (11)
63	441.8	0.0018	H-8→L+4 (15), H-5→L+9 (10), H-4→L+9 (65)
64	439.5	0.0001	H-17→LUMO (72), H-15→LUMO (23)
65	439.4	0.0004	H-17→LUMO (25), H-15→LUMO (66)
66	437.6	0.4145	H-2→L+7 (68)
67	437.2	0.0703	H-30→LUMO (21), H-27→LUMO (23), H-26→LUMO (13), H-25→LUMO (10), H-2→L+7 (17)
68	436.3	0.001	H-18→LUMO (83), H-15→LUMO (10)
69	434.2	0	H-19→LUMO (97)
70	434.0	0.0001	H-10→L+2 (93)
71	433.8	0	H-4→L+5 (92)
72	433.2	0.0037	H-30→LUMO (24), H-26→LUMO (21), H-25→LUMO (38)
73	432.5	0	H-5→L+5 (92)
74	431.1	0.4291	H-11→L+5 (13), H-3→L+5 (87)
75	429.5	0.0038	H-9→L+4 (29), H-6→L+4 (47)
76	429.0	0.0039	H-2→L+8 (97)
77	426.8	0.0045	H-9→L+4 (50), H-6→L+4 (26)
78	426.5	0.0001	HOMO→L+9 (91)
79	426.4	0.0005	H-20→L+1 (92)
80	426.4	0.0002	H-26→LUMO (49), H-25→LUMO (43)
81	424.7	0	H-22→LUMO (95)
82	424.5	0	H-11→L+1 (99)
83	423.1	0	H-21→LUMO (96)
84	422.2	0.0034	H-8→L+4 (62), H-4→L+10 (10)
85	418.8	0.0034	H-30→LUMO (31), H-27→LUMO (51)

86	417.0	0.0314	H-32→LUMO (18), H-28→L+1 (22), H-4→L+10 (22)
87	416.0	2.9505	H-7→L+3 (20), H-5→L+6 (16), H-2→L+3 (11), H-2→L+7 (10)
88	415.5	0.0003	H-24→LUMO (22), H-23→LUMO (74)
89	415.1	0.1689	H-28→L+1 (47), H-4→L+10 (14)
90	414.7	0.0009	H-3→L+7 (100)
91	413.6	0.0005	H-29→LUMO (22), H-24→LUMO (53), H-23→LUMO (21)
92	412.3	0.0001	H-29→LUMO (67), H-24→LUMO (23)
93	411.7	0.0015	H-2→L+9 (94)
94	410.0	0	H-3→L+8 (100)
95	409.7	0.0114	H-5→L+7 (74), H-4→L+7 (20)
96	407.1	0.0025	H-40→LUMO (15), H-32→LUMO (41)
97	404.2	0.004	H-36→LUMO (21), H-5→L+7 (12), H-4→L+7 (50)
98	404.2	0.0022	H-36→LUMO (34), H-4→L+7 (29)
99	403.2	0	H-5→L+8 (75), H-4→L+8 (25)
100	402.8	0	H-14→L+1 (22), H-13→L+1 (78)

References:

1. Maligaspe, E.; Kumpulainen, T.; Subbaiyan, N. K.; Zandler, M. E.; Lemmetyinen, H.; Tkachenko, N. V.; D'Souza, F., *Phys. Chem. Chem. Phys.* **2010**, 7434-7444.